

1 **An early Sox2-dependent gene expression program required for hippocampal** 2 **dentate gyrus development**

3

4 Sara Mercurio, Chiara Alberti, Linda Serra, Simone Meneghini, Jessica Bertolini, Pietro Berico,
5 Andrea Becchetti and Silvia K. Nicolis

6

7 Department of Biotechnology and Biosciences, University of Milano-Bicocca, piazza della Scienza
8 2, 20126 Milano, Italy

9

10 Correspondence: silvia.nicolis@unimib.it, sara.mercurio@unimib.it

11

12

13 **Abstract**

14

15 The hippocampus is a brain area central for cognition. Mutations in the human SOX2 transcription
16 factor cause neurodevelopmental defects, leading to intellectual disability and seizures, together
17 with hippocampal dysplasia. We generated an allelic series of Sox2 conditional mutations in mouse,
18 deleting Sox2 at different developmental stages. Late Sox2 deletion (from E11.5, via Nestin-Cre)
19 affects only postnatal hippocampal development; earlier deletion (from E10.5, Emx1-Cre)
20 significantly reduces the dentate gyrus, and the earliest deletion (from E9.5, FoxG1-Cre) causes
21 drastic abnormalities, with almost complete absence of the dentate gyrus. We identify a set of
22 functionally interconnected genes (Gli3, Wnt3a, Cxcr4, p73 and Tbr2), known to play essential
23 roles in hippocampal embryogenesis, which are downregulated in early Sox2 mutants, and (Gli3
24 and Cxcr4) directly controlled by SOX2; their downregulation provides plausible molecular
25 mechanisms contributing to the defect. Electrophysiological studies of the Emx1Cre mouse model
26 reveal altered excitatory transmission in CA1 and CA3 regions.

27

28

29

30

31 **Introduction**

32

33 The hippocampus is a brain region important for cognition, playing essential roles in learning and
34 in spatial and episodic memory formation. Hippocampus defects (of genetic origin, or acquired) can
35 lead to intellectual disability (ID), deficits of memory formation, and epilepsy (Kandel, Schwartz,
36 & Jessell, 2000).

37 Within the hippocampus, the dentate gyrus (DG) represents the primary input site for excitatory
38 neuronal projections; the major type of DG neurons (granule neurons) are generated by neural stem
39 cells (NSC) that are defined early in development, and continue neurogenesis during embryogenesis
40 and also in postnatal stages, in mice as well as in humans (Berg et al., 2019; Zhong et al., 2020).

41

42 Patients carrying heterozygous loss-of-function mutations in the gene encoding the SOX2
43 transcription factor show a characteristic spectrum of central nervous system (CNS) defects,
44 including hippocampal defects (involving the dentate gyrus), ID, and epilepsy (Fantes et al., 2003;
45 Kondoh H, 2016; Ragge et al., 2005; Sisodiya et al., 2006). Understanding the developmental
46 events and the genetic program controlled by SOX2 during hippocampal embryogenesis therefore
47 provides a key to understand how their perturbation can lead to hippocampal disease (in SOX2-
48 mutant patients and, more in general, in hippocampal defects of genetic origin).

49

50 In mouse, Sox2-dependent hippocampal disease has been previously modelled by conditional
51 mutagenesis (Favaro et al., 2009). Sox2 pan-neural deletion at mid-embryogenesis, via a Nestin-Cre
52 transgene, led to a relatively normal hippocampal development up to birth; at early postnatal stages,
53 however, the hippocampus failed to complete its development, and remained hypoplastic, due to a
54 failure of postnatal DG NSC. The study of SOX2 binding to DNA in NSC proved instrumental in
55 the identification of various Sox2 target genes, playing important roles in the development of
56 different brain regions in vivo, such as the basal ganglia (A. Ferri et al., 2013), the cerebellum
57 (Cerrato et al., 2018), and the visual thalamus (Mercurio et al., 2019).

58

59 While postnatal hippocampal development was perturbed following Nestin-Cre-mediated Sox2
60 deletion, embryonic hippocampal development was, quite surprisingly, very little, if at all, affected
61 in these mutants (Favaro et al., 2009). In principle, this could be due to redundant functions played
62 by other homologous genes of the SoxB family, such as Sox1 and Sox3, coexpressed with Sox2 in

63 the developing neural tube, and reported to function in hippocampal neural stem/progenitor cells
64 (Rogers et al., 2013); alternatively, we reasoned that Sox2 may play non-redundant, very early
65 functions in hippocampal development, that might not be revealed by Nestin-Cre-mediated
66 deletion.

67

68 Here, we generated an allelic series of Sox2 conditional mutations, using Cre transgenes deleting
69 Sox2 at stages earlier than Nestin-Cre: FoxG1-Cre, active from embryonic day (E) 8.5 (Hébert &
70 McConnell, 2000), and Emx1-Cre (Gorski et al., 2002), active from E10.5. We report that early
71 Sox2 deletion leads to drastic defects of hippocampal development, the earlier the deletion, the
72 stronger the phenotype: in Emx1-Cre mutants, hippocampal development is perturbed, but still
73 present, but in FoxG1-Cre mutants, hippocampal development is severely impaired, and the DG
74 essentially fails to develop. We propose that Sox2 sets in motion a very early gene expression
75 program in the hippocampal primordium, required for all of its subsequent development. Indeed,
76 we show that early (but not late) Sox2 deletion reduces the expression of several genes (some of
77 which SOX2-bound), individually characterized by previous studies as master regulators of
78 hippocampal development (and human neurodevelopmental disease), including Gli3, Wnt3a,
79 Cxcr4, Tbr2 and p73, some of which are known to cross-regulate each other.

80

81

82 **Results**

83

84 ***Sox2 is expressed in the primordium of the developing hippocampus and in the adjacent cortical*** 85 ***hem***

86 The transcription factor Sox2 is expressed throughout the neural tube from the beginning of its
87 development (Avilion et al., 2003; Favaro et al., 2009; A. L. Ferri et al., 2004; Mariani et al., 2012).
88 The hippocampus starts to develop around embryonic day (E) 12.5, in the medial wall of the
89 telencephalon, and becomes morphologically recognizable in the following days (Fig. 1A) (Berg et
90 al., 2019; Hodge et al., 2012). A region essential for the formation of the hippocampus is the cortical
91 hem (CH), also known as the hippocampal organizer, identified in mice at E12.5; signaling from
92 the CH is able to organize the surrounding tissue into a hippocampus (Grove, 2008; Mangale et al.,
93 2008). The dentate neural epithelium (DNE), adjacent to the cortical hem (Fig. 1A), contains neural
94 stem cells (NSC), that will generate granule neurons in the hippocampus dentate gyrus (DG)
95 throughout development and, subsequently, in postnatal life (Berg et al., 2019). On the outer side

96 of the neuroepithelium, towards the pia, a population of neurons, called Cajal-Retzius cells (CRC)
97 (Fig. 1A) develops, that will have a key role in the morphogenesis of the hippocampus. NSC and
98 intermediate neural progenitors (INP) will migrate from the DNE, along the dorsal migratory
99 stream (DMS), towards the forming hippocampal fissure (HF), a folding of the meninges that will
100 be invaded by CRC (Fig. 1A).

101 We examined Sox2 expression by *in situ* hybridization (ISH) and immunofluorescence (IF), in the
102 medial telencephalon, from which the hippocampus develops, between E12.5 and E18.5 (Fig. 1B-
103 I). At E10.5 Sox2 is expressed in the whole telencephalon including the dorso-medial region that
104 will give rise to the hippocampus (Fig. 1B). At E12.5, Sox2 is expressed throughout the
105 neuroepithelium in the medial telencephalic wall and it is enriched in the CH region (Fig. 1C); at
106 E15.5, expression persists in the neuroepithelium, and is detected in the DMS and in the fimbria (a
107 CH derivative) (Fig. 1D). Just before birth, at E18.5, Sox2 expression is detected in the developing
108 DG (Fig. 1E,E').

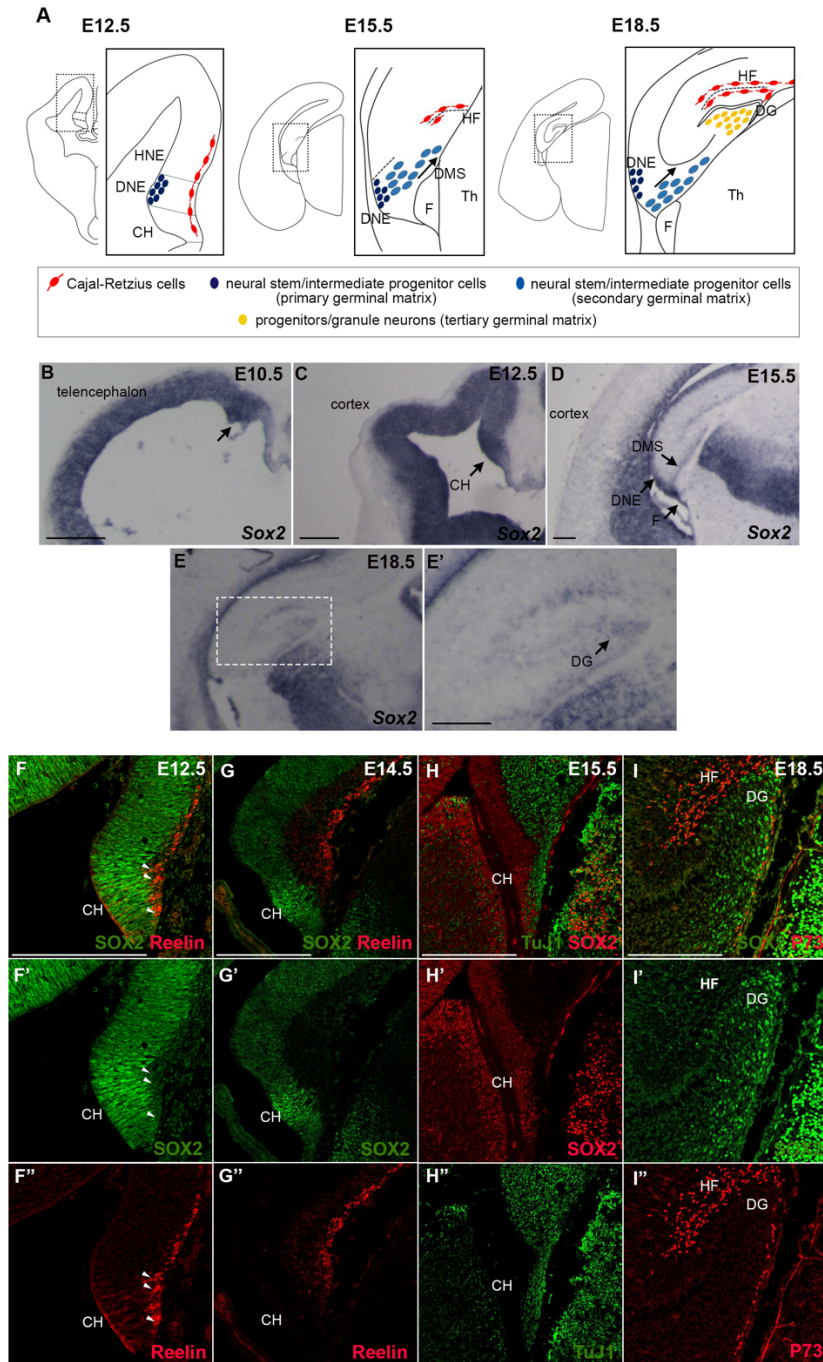
109 We then performed co-immunohistochemistry experiments with antibodies against SOX2, and
110 markers of more differentiated cell types: CR cells markers Reelin and P73 (Fig. 1F,G,I) and the
111 pan-neuronal marker TuJ1 (Fig. 1H). While SOX2 was detected in all cells within the
112 neuroepithelium, as expected, we detected no or very little (Fig. 1F arrowheads) overlap with TuJ1,
113 Reelin, or p73 (Fig. 1 F-I). Moreover, to test if Sox2 is expressed in the progenitors of CRC, we
114 turned on EYFP in Sox2-expressing cells of the early telencephalon before CRC differentiation
115 started, at E9.5 (via a Sox2-CreERT2 transgene and a lox-stop-lox reporter of Cre activity, Fig. S1),
116 and found that these cells differentiated into Reelin-expressing CRC in the hippocampal fissure and
117 the cortex (Fig. S1).

118 Thus, Sox2 expression in the developing hippocampus and CH is present mainly in undifferentiated
119 neuroepithelial cells (including CRC precursors), and becomes extinguished in differentiation.

120

121 ***Sox2 early ablation (FoxG1-Cre) prevents the development of the hippocampal dentate gyrus,***
122 ***and severely compromises hippocampal embryogenesis***

123 Sox2 is required for postnatal development of the hippocampus, in particular to maintain NSC in
124 the DG (Favaro et al., 2009); however, whether Sox2 has a role in hippocampus embryogenesis was
125 not known. To address this question, we generated three different conditional knock-outs, to ablate
126 Sox2 at different time points of telencephalon development. Specifically, we crossed a Sox2 floxed
127 allele (Favaro et al., 2009) with the following Cre lines: FoxG1-Cre, deleting between E8.5 and



128

129 **Figure 1**
 130 **Sox2 expression in the dorsal telencephalon.**

131 (A) Schematic representation of the development of the hippocampus in the dorsal telencephalon. (B-E) *In*
 132 *situ* hybridization for *Sox2* on coronal section of mouse brains at E10.5 (B) E12.5 (C), E15.5 (D), E18.5 (E).
 133 Arrows indicate *Sox2* expression in the developing hippocampus in particular in the dorsal telencephalon in
 134 (B), in the cortical hem (CH) in (C), in the dorsal migratory stream (DMS) in (D) and in the dentate gyrus
 135 (DG) in (E'). (F-I) Immunofluorescence of *Sox2* (F-I), of markers of CRC, Reelin (F,G) and P73 (I), and of
 136 a marker of differentiating neurons TuJ1 (H). Representative single optical confocal sections are shown.
 137 Scale bars 200 μ m.

138 CH, cortical hem; DNE, dentate neuroepithelium; HNE, hippocampal neuroepithelium; DMS, dentate
 139 migratory stream; HF, hippocampal fissure; DG, dentate gyrus; F, fimbria; Th, thalamus.

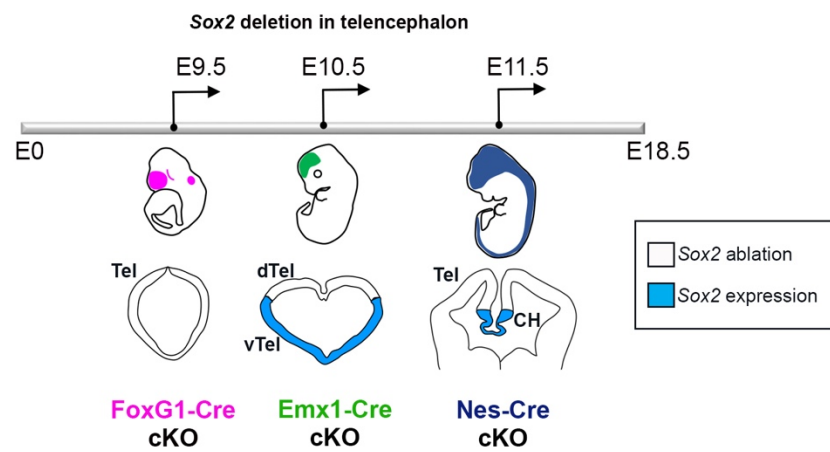
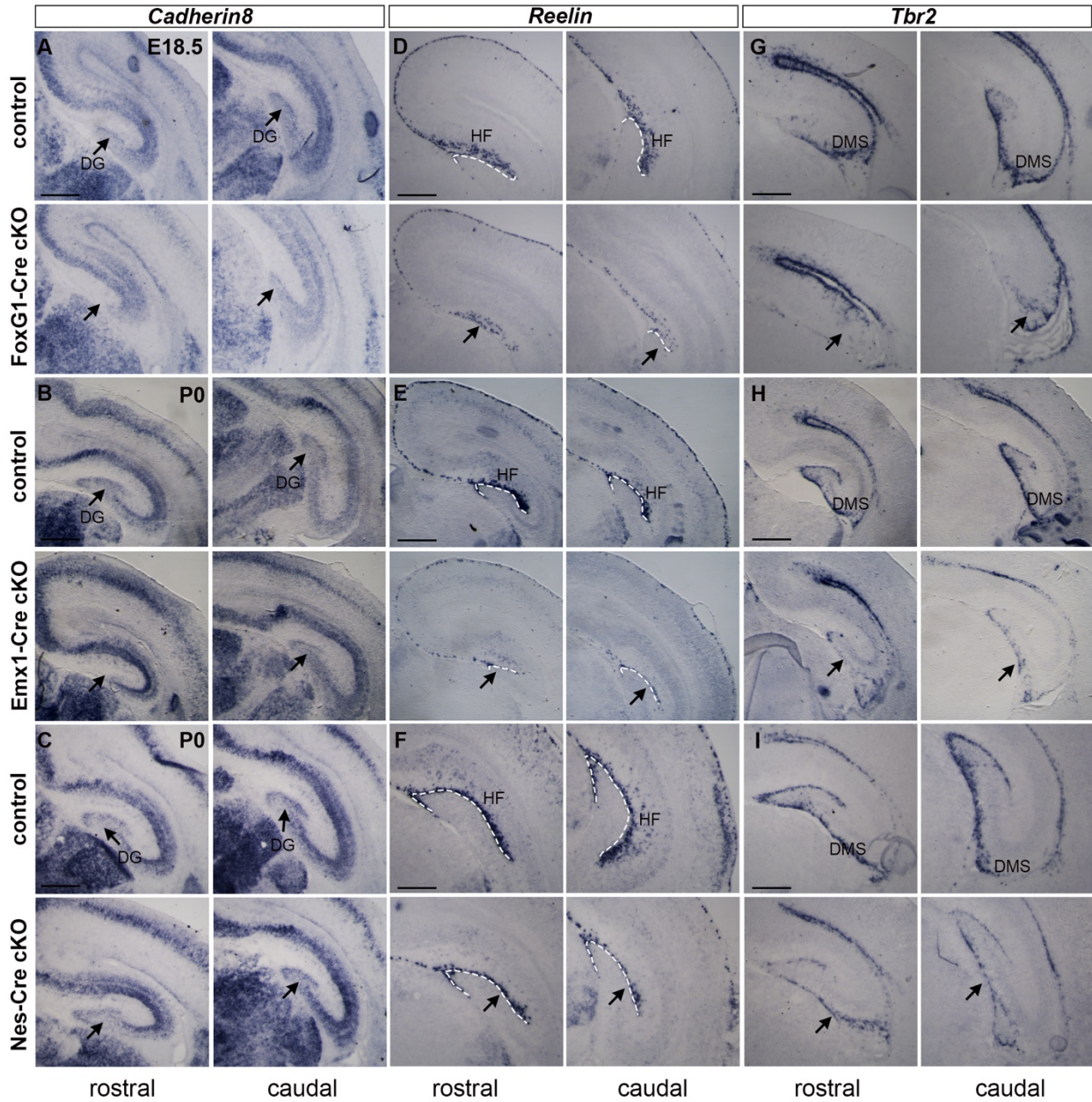
140 E9.5 (A. Ferri et al., 2013; Hébert & McConnell, 2000), Emx1-Cre, deleting after E10.5 (Gorski et
141 al., 2002), and Nestin-Cre, deleting after E11.5 (Tronche et al., 1999). The resulting conditional
142 knock-outs (Sox2^{flox/flox};FoxG1-Cre; Sox2^{flox/flox};Emx1-Cre; Sox2^{flox/flox};Nestin-Cre) will be called
143 FoxG1-Cre cKO, Emx1-Cre cKO and Nestin-Cre cKO respectively, from now onwards. As
144 expected, complete Sox2 deletion is observed already at E9.5 in FoxG1-Cre cKO (in the whole
145 telencephalon), and at E10.5 in Emx1-Cre cKO (in the dorsal telencephalon); in the Nestin-Cre
146 cKO, deletion occurs after E11.5 (Favaro et al., 2009, Ferri et al., 2013, and data not shown).

147

148 We initially explored hippocampus development in the different mutants at the end of gestation
149 (E18.5; P0), performing ISH with probes identifying hippocampal structures and cell types (Fig. 2).
150 ISH for a general marker of the developing hippocampus, Cadherin 8 (Korematsu & Redies, 1997),
151 shows that, at the end of gestation (E18.5, P0) the DG appears little, if at all, affected in the Nestin-
152 Cre cKO (Fig. 2C), as expected (Favaro et al., 2009). However, in the Emx1-Cre cKO, the DG is
153 greatly reduced, in particular anteriorly (Fig. 2B); remarkably, in the FoxG1-Cre cKO, the DG
154 appears to be almost absent (Fig. 2A).

155 At the end of gestation, CRC, expressing Reelin (D'Arcangelo et al., 1995), and INP, expressing
156 Tbr2 (Hodge et al., 2013), have a characteristic organization in the hippocampus: CRC are localized
157 around the HF, while INP have migrated from the DNE, by the ventricle, along the DMS, have
158 reached the HF and are found below the CRC layer (see Fig. 1A). In the FoxG1-Cre cKO, Reelin
159 expression (marking CRC) is greatly reduced, and a HF is not observed (Fig. 2D); in Emx1-Cre
160 cKO, Reelin is reduced, but the HF is visible (Fig. 2E), and in Nestin-Cre cKO Reelin appears
161 slightly reduced, but with a normal-looking distribution around the HF (Fig. 2F). Similarly, Tbr2
162 expression is greatly reduced in FoxG1-Cre cKO; an initial dorsal migratory stream is visible, but
163 no DG is observed (Fig. 2G). Instead, in Emx1-Cre cKO, Tbr2-positive INP have reached the HF,
164 but their abundance is greatly reduced (Fig. 2H). On the other hand, in Nestin-Cre cKO, Tbr2-
165 positive INP appear to have completed their migration, and their abundance seems only slightly, if
166 at all, reduced (Fig. 2I).

167 To summarize, Sox2 ablation by E9.5 in the telencephalon in FoxG1-Cre cKO results, by the end of
168 gestation, in lack of DG formation, accompanied by a missing HF. Ablation just a day later, in
169 Emx1-Cre cKO, has much less dramatic effects: a hippocampal fissure forms, though CRC and INP
170 are reduced and the DG is much smaller compared to controls. Nestin-Cre cKO appear much less, if
171 at all, affected, as previously published (Favaro et al., 2009).



173 **Figure 2**

174 **Hippocampus development is affected by Sox2 loss, the early Sox2 is ablated the stronger the**
175 **phenotype observed.**

176 *In situ* hybridization for *Cadherin8* (A-C), *Reelin* (D-F) and *Tbr2* (G-I) on coronal sections of control and
177 Sox2 FoxG1-Cre cKO brains at E18.5 (A,D,G), control and Emx1-Cre cKO brains at P0 (B,E,H) and control
178 and Nes-Cre cKO brains at P0 (C,F,I). At least 3 controls and 3 mutants were analyzed for each probe. A
179 schematic representation of the timing of Sox2 ablation with the different Cre lines is at the bottom. Scale
180 bars 200 μ m.

181 DG, dentate gyrus; HF, hippocampal fissure; DMS, dentate migratory stream; Tel, telencephalon; dTel,
182 dorsal telencephalon; vTel, ventral telencephalon; CH, cortical hem.

183

184 ***Neural progenitors, differentiated neurons and radial glia are affected by Sox2 loss***

185 We then characterized the development of specific hippocampal cell types in the most affected

186 (FoxG1-Cre) mutants. Key for the morphogenesis of the hippocampus is the radial glia (RG)

187 scaffold known to be required for the DMS to reach its final destination in the forming DG (Li,

188 Kataoka, Coughlin, & Pleasure, 2009). By immunohistochemistry for GFAP, recognizing RG, at

189 E18.5, we find that the RG scaffold in FoxG1-Cre cKO is completely disorganized (Fig. 3A). No

190 morphologically identifiable DG is present, and the few RG found have random organization (Fig.

191 3A, arrows). At this same stage, different neuronal populations are normally found in the

192 hippocampus: granule neurons in the DG, and pyramidal neurons forming the CA1, CA2 and CA3

193 regions. We performed ISH for NeuroD1, a marker of differentiated neurons; in FoxG1-Cre cKO,

194 while NeuroD1-positive cells in the CA regions are present, NeuroD1-positive cells in the DG,

195 abundant in controls, are almost absent in the mutant (Fig. 3B).

196 In the DG, at this stage, neural stem/progenitor cells, marked by the expression of the Hes5 gene

197 (Basak & Taylor, 2007), are normally present (see Fig. 3C, controls); in FoxG1-Cre cKO, however,

198 very few Hes5-positive cells are found (Fig. 3C).

199 In conclusion, early Sox2 loss in the telencephalon (FoxG1-Cre cKO) appears to lead to later

200 reduction of both differentiated neurons and proliferating neural progenitors; in addition, the radial

201 glia scaffold is completely disorganized.

202

203 ***The formation of the hippocampal fissure and the dentate migration require Sox2 expression***

204 ***from early developmental stages***

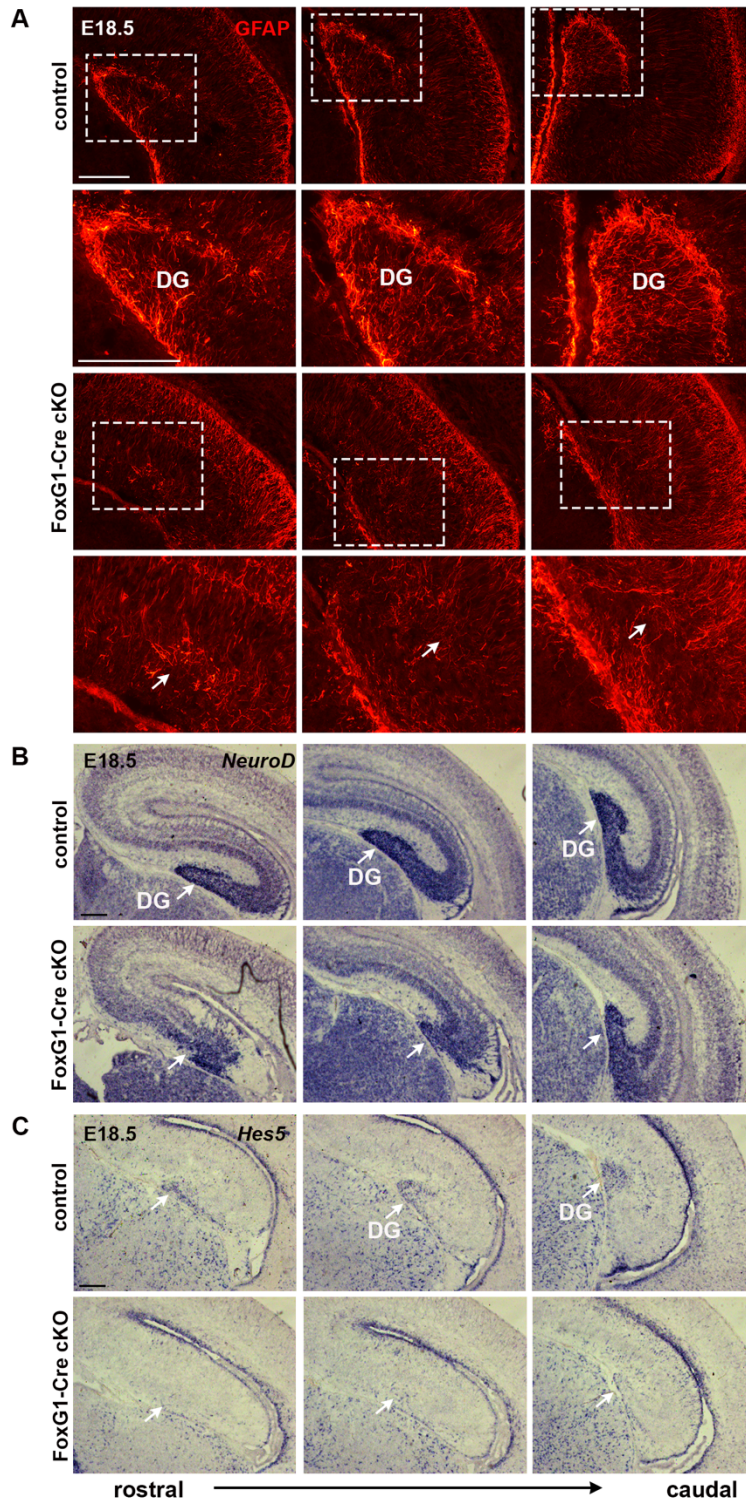
205 After having identified the hippocampal defects present, in our mutants, at the end of gestation, we

206 examined earlier developmental stages, to define the developmental history of the defects. We

207 focused in particular on the FoxG1-Cre mutant, showing the most pronounced abnormalities (see

208 Fig. 2).

209



210
211
212
213
214
215
216
217
218

Figure 3

Radial glia formation, neuronal differentiation and neural stem cells formation is severely affected in FoxG1-Cre cKO.

(A) GFAP immunofluorescence at E18.5 on coronal sections of control and FoxG1-Cre cKO hippocampi (controls n=6, mutants n=4). (B,C) *In situ* hybridization at E18.5 for *NeuroD* (B) (controls n=4, mutants n=3) and *Hes5* (C) (controls n=2, mutants n=2) on coronal sections of control and FoxG1-Cre cKO hippocampi. Arrows indicate the underdeveloped dentate gyrus (DG) in cKO. Scale bars 200 μ m.

219 A defect in distribution of CRC (marked by Reelin) and INP (marked by Tbr2) is apparent, at the
220 end of gestation, in Sox2 FoxG1-Cre and Emx1-Cre cKO (Fig. 2D,E,G,H). What happens in the
221 first steps of the development of the hippocampus to CRC and INP in these mutants? We addressed
222 this question by ISH with markers for these cell types at early developmental stages, in FoxG1-Cre
223 (Early) cKO embryos (Fig. 4). We also examined the expression of Cxcr4, a chemokine receptor
224 expressed in INP and neuroblasts in the DMS and in CRC, and its ligand Cxcl12, expressed by the
225 meninges, and required for the migration of INP and CRC (Berger, Li, Han, Paredes, & Pleasure,
226 2007; Borrell & Marin, 2006; Hodge et al., 2013; Li et al., 2009); we also examined P73, a P53
227 homolog, expressed by CRC and important for hippocampal fissure and DG formation (Meyer et
228 al., 2004; Meyer et al., 2019).

229
230 At E12.5, Tbr2 is expressed, in controls, by INP in the DNE and in CR cells towards the pia (Fig.
231 4A); in the FoxG1-Cre cKO mutant, whereas Tbr2 expression in CRC (towards the pia, arrow)
232 appears present, expression in the DNE is not detected (Fig. 4A). This might reflect a loss of Tbr2-
233 expressing INP; however, we do not observe changes in the number of proliferating cells in this
234 region at E12.5 by EdU labelling (Fig. S2), suggesting that at least some INP remain, but express
235 less Tbr2 or are mislocalized. P73, Reelin and Cxcr4 expression appears unaltered in mutants
236 compared to controls at this stage (Fig. 4B-D).

237
238 At E14.5, P73 and Reelin expression marks, in controls, CRC in the medial telencephalic wall
239 region where hippocampal morphogenesis will soon begin (Fig. 4E,F, arrow); in the mutant, a
240 strong reduction of P73 and Reelin expression is observed (Fig. 4E,F, arrow). Of note, this
241 reduction is detected specifically in the CH of FoxG1-Cre cKO (Fig. 4E,F), even though Sox2 is
242 ablated in the whole telencephalon. At this stage, also Cxcr4 expression in CRC appears reduced in
243 the CH of FoxG1-Cre cKO (Fig. 4G).

244
245 At E16.5, in controls, strong P73 and Reelin expression marks the hippocampal fissure (HF),
246 defining the beginning of overt hippocampal morphogenesis (Fig. 4H,I); in sharp contrast, this
247 expression is not seen or greatly reduced in the mutant (Fig. 4H,I). Cxcl12 is also expressed, in the
248 control, in the developing HF, and its expression is also lost in the mutant (Fig. 4K).

249 Concomitantly, Cxcr4 expression in the hippocampus primordium (HP) is also reduced (Fig. 4J).
250 These data point to a failure to initiate proper HF development in the mutant.

251 Interestingly, at E16.5, P73, Reelin and Cxcr4 expression is reduced throughout the telencephalon in
252 FoxG1-Cre cKO (Fig. 4).

253

254 At E18.5, P73 marks the HF in controls, but its expression is completely absent in the FoxG1-Cre
255 cKO brain, indicating a complete depletion of P73-positive CH-derived CRC (Fig. 4L). Cxcr4
256 expression in the DG and Cxcl12 expression in the HF is also greatly reduced in the mutant,
257 confirming a severe abnormality of the mutant hippocampus at the end of gestation (Fig. 4M,N).
258 In conclusion, the defects detected, at the end of gestation, in FoxG1-Cre mutants originate early in
259 development, with a failure, at early stages, to develop a HF and migrating DNE cells in these
260 mutants.

261

262 ***Genes essential for hippocampal development are downregulated following early (FoxG1-Cre***
263 ***cKO), but not late (Emx1-Cre cKO, Nestin-Cre cKO), Sox2 deletion***

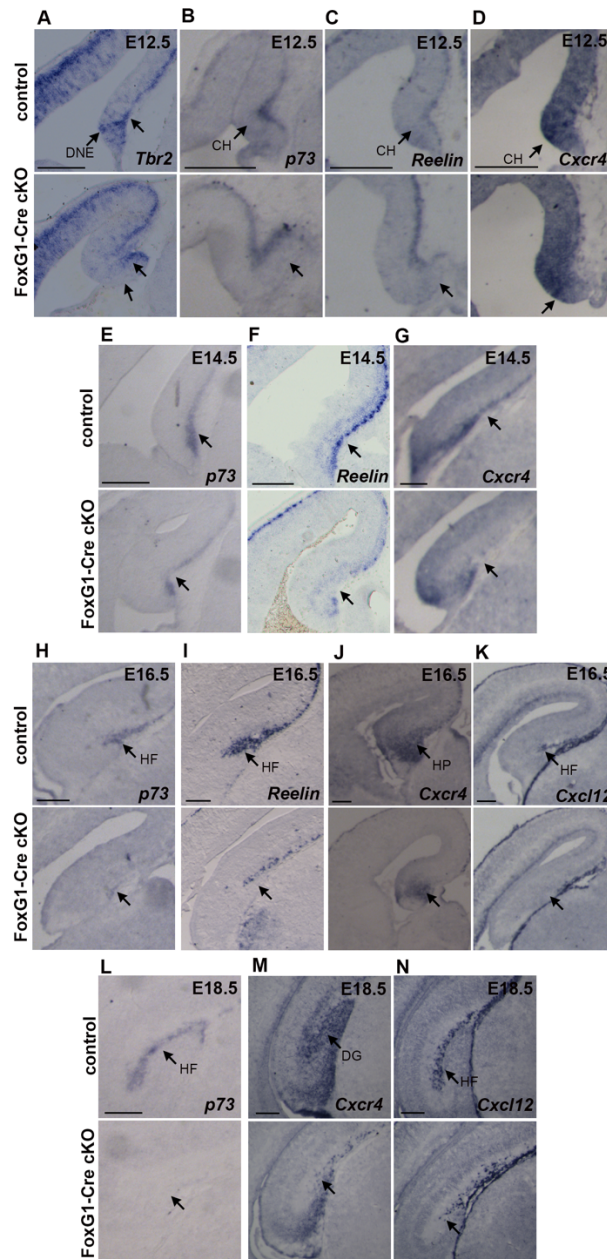
264 Having observed that early Sox2 mutants (in particular FoxG1-Cre cKO) show severely defective
265 hippocampal development, we searched for Sox2-regulated downstream genes, whose deregulation
266 in mutants could explain the observed defects. We compared the expression of several candidate
267 genes in mutants and controls, at E12.5, a stage preceding the observed abnormalities (clearly
268 observed, in mutants, from E14.5, when hippocampal morphogenesis begins). Having observed that
269 the defects in early Sox2 mutants (FoxG1-Cre cKO) are much more severe than those arising in
270 later (Emx1-Cre and Nestin-Cre cKO) mutants, we reasoned that genes downstream to Sox2, that
271 are functionally relevant for these early defects, should show altered expression in early (FoxG1-
272 Cre) mutants, but not, or less, in later mutants (Emx1-Cre; Nestin-Cre).

273 We thus investigated the expression of genes, representing candidate mediators of Sox2 function, in
274 early and late mutants, by ISH.

275

276 Prime candidate genes to mediate defective hippocampal development in early Sox2 mutants
277 include genes encoding signalling molecules, expressed in the CH.

278 Key signaling molecules secreted by the CH and required for hippocampus formation are
279 components of the Wnt pathway; in fact, Wnt3a knock-out results in a complete loss of the
280 hippocampus (Lee, Tole, Grove, & McMahon, 2000). We analyzed what happens, at E12.5, to the
281 expression of Wnt3A in the three Sox2 cKO. We found that Wnt3A is severely downregulated
282 specifically in the CH of FoxG1-Cre cKO (Fig. 5A), but only slightly downregulated in Emx1-Cre
283 cKO (Fig. 5B), while it is only very mildly, if at all, reduced at this stage in the Nestin-Cre cKO



284

285 **Figure 4**
 286 **Expression of genes important for the development of the hippocampus is affected by Sox2 loss in**
 287 **FoxG1-Cre cKO.**

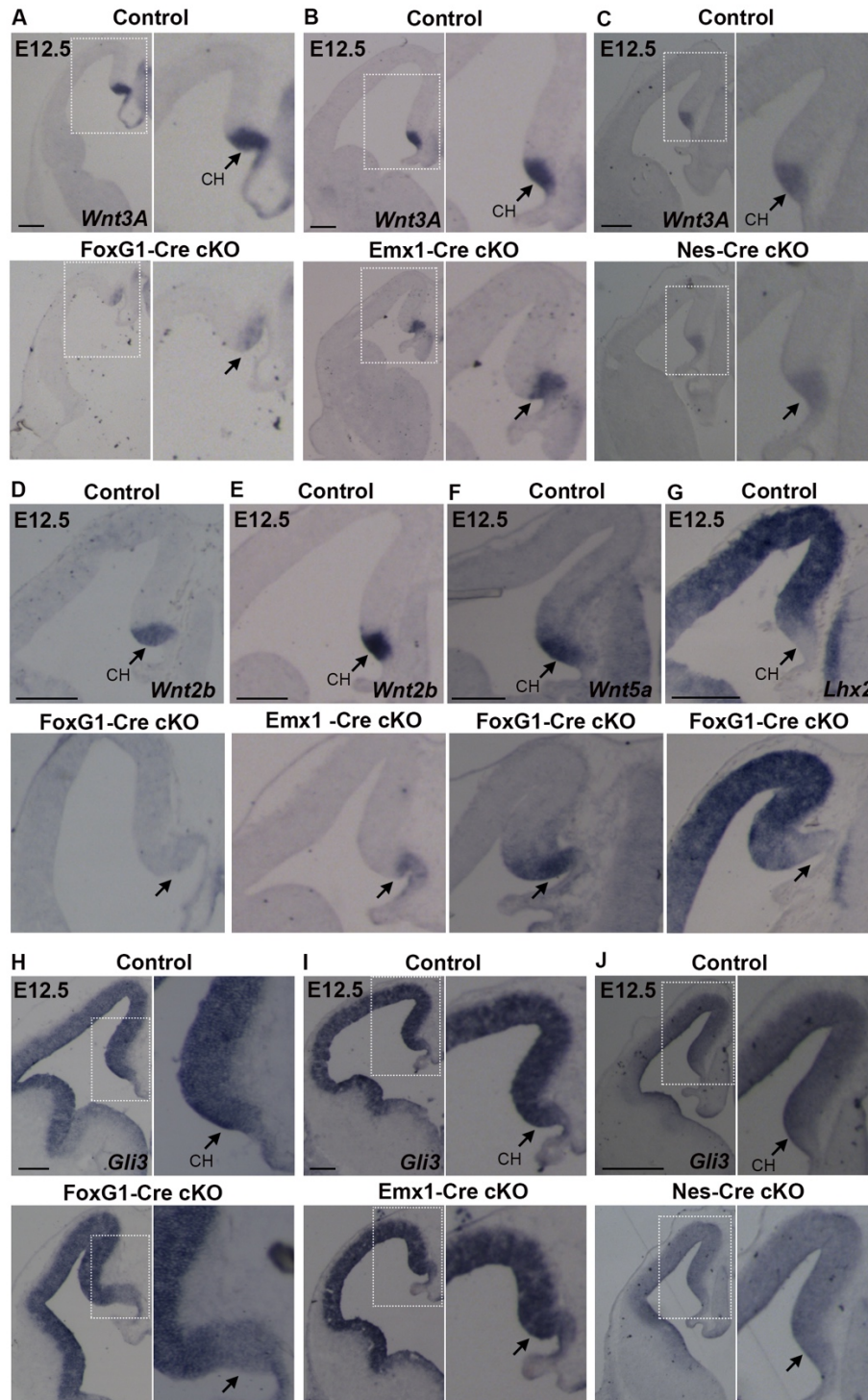
288 (A-D) *In situ* hybridization at E12.5 on coronal sections of control and FoxG1-Cre cKO dorsal
 289 telencephalons for *Tbr2* (controls n=10, mutants n=10) (A), *P73* (controls n=3, mutants n=3) (B), *Reelin*
 290 (controls n=7, mutants n=6) (C) and *Cxcr4* (controls n=7, mutants n=7) (D). (E-G) *In situ* hybridization at
 291 E14.5 on coronal sections of control and FoxG1-Cre cKO brains for *P73* (controls n=3, mutants n=3) (E),
 292 *Reelin* (controls n=7, mutants n=5) (F) and *Cxcr4* (controls n=3, mutants n=3) (G). (H-K) *In situ*
 293 hybridization at E16.5 on coronal sections of control and FoxG1-Cre cKO hippocampi for *P73* (controls
 294 n=2, mutants n=2) (H), *Reelin* (controls n=6, mutants n=5) (I), *Cxcr4* (controls n=5, mutants n=4) (J) and
 295 *Cxcl12* (controls n=4, mutants n=3) (K). (L-N) *In situ* hybridization at E18.5 on coronal sections of control
 296 and FoxG1-Cre cKO hippocampi for *P73* (controls n=3, mutants n=3) (L), *Cxcr4* (controls n=5, mutants
 297 n=4) (M) and *Cxcl12* (controls n=5, mutants n=4) (N). Arrows indicate the downregulation of expression in
 298 the mutant cortical hem (CH), dentate neuroepithelium (DNE), hippocampal primordium (HP), dentate gyrus
 299 (DG) and hippocampal fissure (HF). Scale bars 200 μm.

300 (Fig. 5C). We analyzed the expression of another Wnt family member, Wnt2b in FoxG1-Cre cKO
301 and Emx1-Cre cKO. While Wnt2b was strongly downregulated in the CH of FoxG1-Cre cKO (Fig.
302 5D), it was only slightly downregulated in the CH of Emx1-Cre cKO compared to controls (Fig.
303 5E). Wnt5A, another Wnt family member normally expressed in the CH, was instead expressed in
304 the CH of FoxG1-Cre cKO (Fig. 5F), indicating that the CH, as a structure, is present in these
305 mutants, though it fails to express Wnt3a and Wnt2b. Interestingly, expression of the transcription
306 factor Lhx2, a marker of the cortex which is not expressed in the cortical hem, has a normal
307 expression pattern in FoxG1-Cre cKO, including an Lhx2-non-expressing neuroepithelial region,
308 suggesting that a CH is present in these mutants (Fig. 5G).
309 In conclusion, expression of components of the Wnt pathway known to be involved in the
310 development of the hippocampus is strongly downregulated in the CH of FoxG1-Cre cKO, but not
311 of Emx1-Cre cKO and Nestin-Cre cKO.

312
313 Other key genes for hippocampus formation include Gli3, encoding a transcription factor acting as
314 a nuclear effector in the Shh signaling pathway. The knockout of Gli3 impairs the development of
315 the hippocampus, where DG development is as severely affected as in our Sox2 early (FoxG1-Cre
316 cKO) mutants. Of note, Gli3 acts, in hippocampal development, by regulating expression of
317 components of the Wnt pathway (Grove, Tole, Limon, Yip, & Ragsdale, 1998). We found that Gli3
318 expression is specifically downregulated in the CH (though not in the cortex) of FoxG1-Cre cKO,
319 but not of Emx1-Cre cKO and Nestin-Cre cKO (Fig. 5H-J).

320
321 Recent work from our laboratory identified SOX2 binding sites in an intron of the Gli3 gene in
322 NSC cultured from the mouse forebrain; further, this intronic region is connected to the Gli3
323 promoter by a long-range interaction mediated by RNAPolIII ((Bertolini et al., 2019) and Fig. 6A).
324 A DNA segment, overlapping the SOX2 peak, drives expression of a lacZ transgene to the
325 embryonic mouse forebrain ((Visel et al., 2009) and <https://enhancer.lbl.gov>) (Fig. 6A). We found
326 that this Sox2-bound region, when connected to a minimal promoter and a luciferase reporter gene,
327 and transfected in Neuro2a cells, is activated by increasing doses of a cotransfected Sox2-
328 expressing vector in a dose-dependent way (Fig. 6B).

329
330 Cxcr4, downregulated in early (FoxG1Cre) Sox2 mutants at E14.5 (Fig. 4G), is also functionally
331 involved in the development of the hippocampus (Discussion). Of note, an enhancer active in the
332 developing brain, located within an intron of the Dars gene, but connected to the Cxcr4 gene



333

334

335 **Figure 5**

336 **Expression of key molecules for hippocampal development is downregulated in the cortical hem of**
337 **FoxG1-Cre cKO but mildly or not affected in Emx1- Cre or Nes-Cre cKO.**

338 *In situ* hybridization at E12.5 for *Wnt3A* (A-C), *Wnt2b* (D,E), *Wnt5A* (F), *Lhx2* (G), *Gli3* (H-J) on control and FoxG1-Cre cKO (A,D,F,G,H), Emx1-Cre cKO (B,E,I) and Nes-Cre cKO (C,J) coronal brain sections.

340 Arrows indicate the cortical hem (CH). At least 3 controls and 3 mutants were analyzed for each probe.

341 Scale bars 200 μ m.

342
343
344
345
346
347
348
349
350
351
352
353
354
355
356
357
358
359
360
361
362
363
364
365
366
367
368
369
370
371
372
373
374

promoter by a long-range interaction in brain-derived NSC chromatin, is bound by SOX2 in these cells (Bertolini et al., 2019) (Fig. 6C).

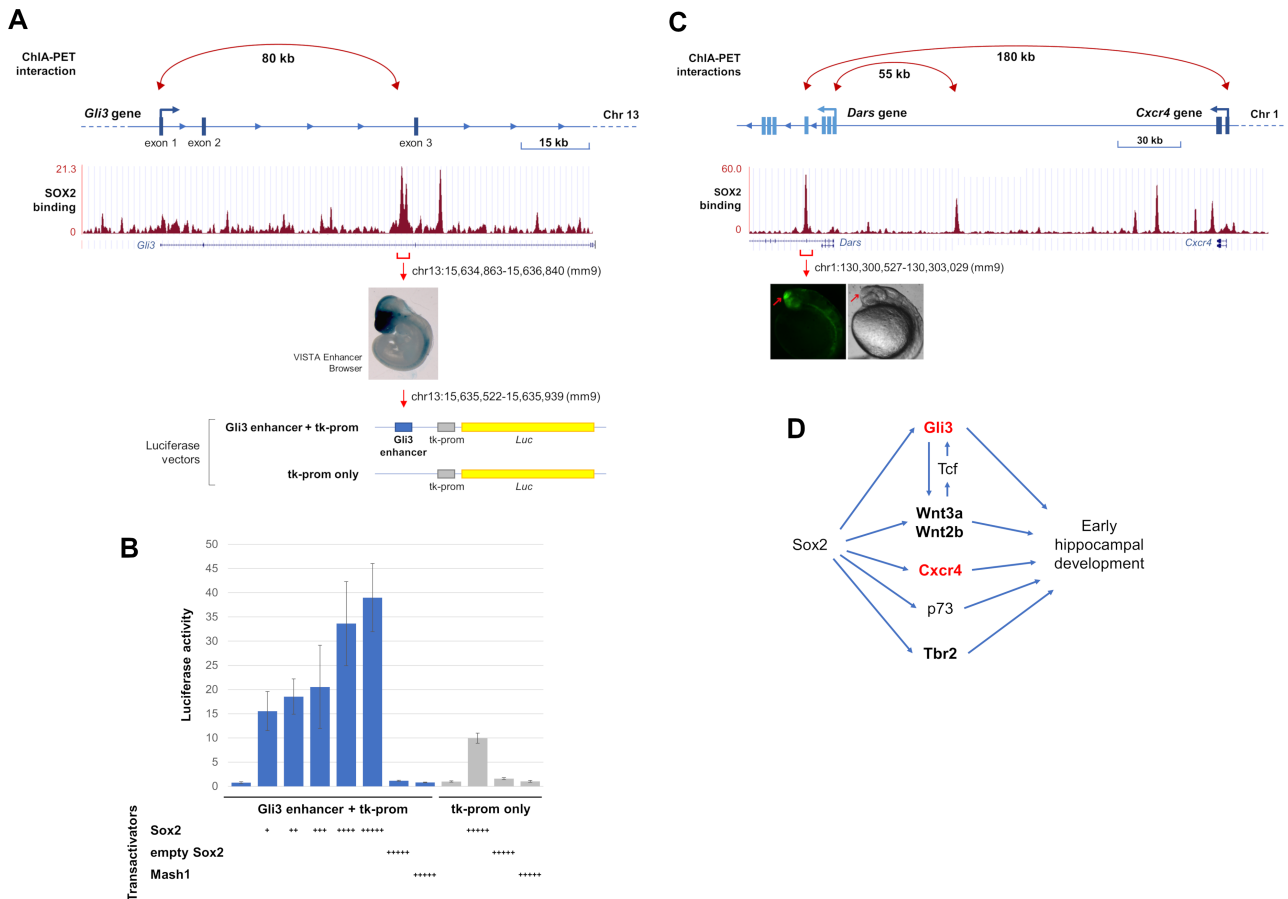
In conclusion, Sox2 early ablation leads to reduced expression, particularly in early (FoxG1-Cre) mutants, of several genes key to hippocampal development, some of which are directly bound and regulated by SOX2; some of these genes (Gli3, Wnt3a) are also known to functionally regulate each other (see Discussion). These genes may thus be considered as part of a Sox2-dependent gene regulatory network, controlling hippocampal development (Fig. 6D; see Discussion).

Emx1-Cre mediated Sox2 ablation alters the excitatory input in CA3 and CA1 pyramidal neurons

We also wished to ask about the consequences of Sox2 early loss on the physiological functioning of the postnatal hippocampus.

As illustrated earlier (Fig. 2A, 2B), early Sox2 loss causes DG hypoplasia, most severe in FoxG1-cKO mutants, but clearly present also in Emx1-Cre cKO mice. Since FoxG1-cKO are perinatally lethal (A. Ferri et al., 2013), we performed physiology studies on Emx1-cKO mutants. We addressed, in particular, the function of CA3 and CA1 pyramidal neurons, central to hippocampal circuitry and relatively spared, morphologically at least, in our mutants (in comparison to the severely hypoplastic DG).

The DG receives its main extrinsic input from the entorhinal cortex and is the first hippocampal station of the classical trisynaptic pathway: entorhinal cortex → DG granule cells → CA3 pyramidal neurons → CA1 pyramidal neurons. The DG projects exclusively to CA3 through mossy fibers. In turn, CA3 projects to CA1 through Schaffer collaterals (Witter & Amaral, 2004). Hence, we investigated whether the hypoplastic DG in our Emx1-Cre mutants could alter signal transfer to CA3 and CA1. This hypothesis was tested by studying intrinsic excitability and excitatory transmission in CA3/CA1 pyramidal neurons. These were first identified by their typically large pyramidally-shaped soma (~20 μm diameter, in CA3), and then further distinguished by their action potential firing. We focused on regular-spiking pyramidal neurons, the widest population, characterized by slow firing with modest adaptation and excitability properties consistent with literature on CA1-CA3 neurons in mice (e.g., (Hunt, Linaro, Si, Romani, & Spruston, 2018; Venkatesan, Liu, & Goldfarb, 2014)). A typical example is shown in Fig. 7A. The excitability features of pyramidal neurons from control and mutant mice are shown in Supplementary Table 1,



375

376

377

Figure 6

378

SOX2 acts on distal enhancers and on long-range enhancer-promoter interactions of several genes key to hippocampal development, and activates a Gli3 intronic enhancer in a dose-dependent way

379

(A) Diagram of the *Gli3* gene, and SOX2-binding profile across the *Gli3* locus in NSC (ChIPseq data from (Bertolini et al., 2019)). A Sox2-dependent 80kb long-range interaction connects the *Gli3* promoter with a SOX2-bound region, in the second intron (ChIA-PET data from (Bertolini et al., 2019)). This region acts as a brain-specific enhancer in E10.5 mouse embryo (image from <https://enhancer.lbl.gov/>); it was cloned into the depicted luciferase vector, upstream to a minimal tk promoter, to address its responsiveness to Sox2.

384

(B) Enhancer activation assay in Neuro2a cells transfected with the constructs in (A): *Gli3* enhancer + tk-promoter (blue histograms), or tk-promoter only (grey histograms). Cotransfection of these constructs with increasing amounts of a Sox2-expressing vector (Sox2, X axis), but not of a control “empty” vector (empty Sox2), or a Mash1-expressing-vector (Mash1), resulted in dose-dependent increase of luciferase activity (Y axis) driven by the *Gli3* enhancer + tk-prom vector, but not the tk-prom only vector. The molar ratios, compared with the luciferase vector (set at 1) were: +, 1:0.050; ++, 1:0.075; +++, 1:0.125; +++, 1:0.25; +++++, 1:0.5. Results are represented as fold-change increase in activity compared with the tk-prom only vector, which is set at 1. Values are the mean of two (for Sox2+ and Sox2++) or three (other samples) independent experiments carried out in triplicate. Error bars represent standard deviation.

389

(C) Diagram of the *Cxcr4* gene, reporting SOX2 binding and Sox2-dependent long-range interactions in NSC (as in A for *Gli3*; data from (Bertolini et al., 2019)). Note that the *Cxcr4* promoter is connected to a SOX2-bound region within the intron of a different gene, *Dars*; this region acts as a brain-specific enhancer in transgenic zebrafish embryos (picture from (Bertolini et al., 2019)).

394

(D) A model depicting the activation, by Sox2, of different genes key to hippocampal development (present paper), some of which cross-regulate each other; in red, direct SOX2 targets; in bold, early expressed hippocampal regulators, downregulated already at early stages in Sox2 mutants (see Discussion).

398

399

400

401

402 while the stimulus/frequency relations are shown in [Fig. 7B](#). Overall, little difference was observed
403 in intrinsic excitability between mutant and control mice, in both CA1 and CA3.

404 In these neurons, we recorded the spontaneous excitatory post-synaptic currents (EPSCs) for 10
405 min after reaching the whole-cell configuration, at -68 mV. Spontaneous EPSCs reflect the overall
406 excitatory input impinging on a given pyramidal neuron. Typical EPSC traces from CA3 pyramidal
407 neurons are shown in [Fig. 7C](#), for controls and mutants. Somewhat surprisingly, EPSC frequencies
408 in CA3 displayed a ~30% increase in mutant animals compared to the controls ([Fig. 7E](#)). On the
409 contrary, the average EPSC median amplitudes were not different between control and mutant mice
410 ([Fig. 7E](#)). Moreover, the EPSC amplitudes obtained from all control and mutant cells were pooled
411 in [Fig. 7F](#). The amplitude distributions of the two genotypes were compared with KS test, which
412 revealed no significant difference.

413 Next, we studied the excitatory input onto CA1, which is the last station of the hippocampal serial
414 pathway of information transfer. Typical EPSC traces are shown in [Fig. 7D](#) for control and mutant.
415 As expected (Traub, Jefferys, & Whittington, 1999), the overall EPSC frequency and amplitude
416 tended to be smaller in CA1, compared to CA3. The average EPSC frequencies in CA1 are reported
417 for control and mutant mice in [Fig. 7G](#). Data reveal an approximately 50% reduction in mutant
418 animals compared to the controls. Once again, little difference between genotypes was observed in
419 the EPSC amplitudes ([Fig. 7G, H](#)).

420 In conclusion, CA3/CA1 pyramidal neuron firing or EPSC amplitudes were not altered in *Emx1-*
421 *Cre* cKO mice, arguing against a direct effect of the mutation on the synaptic machinery or intrinsic
422 excitability, which is consistent with the lack of expression of *Sox2* in these neurons (data not
423 shown). However, EPSC frequency increased in CA3 and was approximately halved in CA1 of
424 mutant mice, suggesting that excitatory signal transfer along the canonical trisynaptic pathway was
425 unbalanced as a consequence of the major impairment of DG development produced by early *Sox2*
426 ablation.

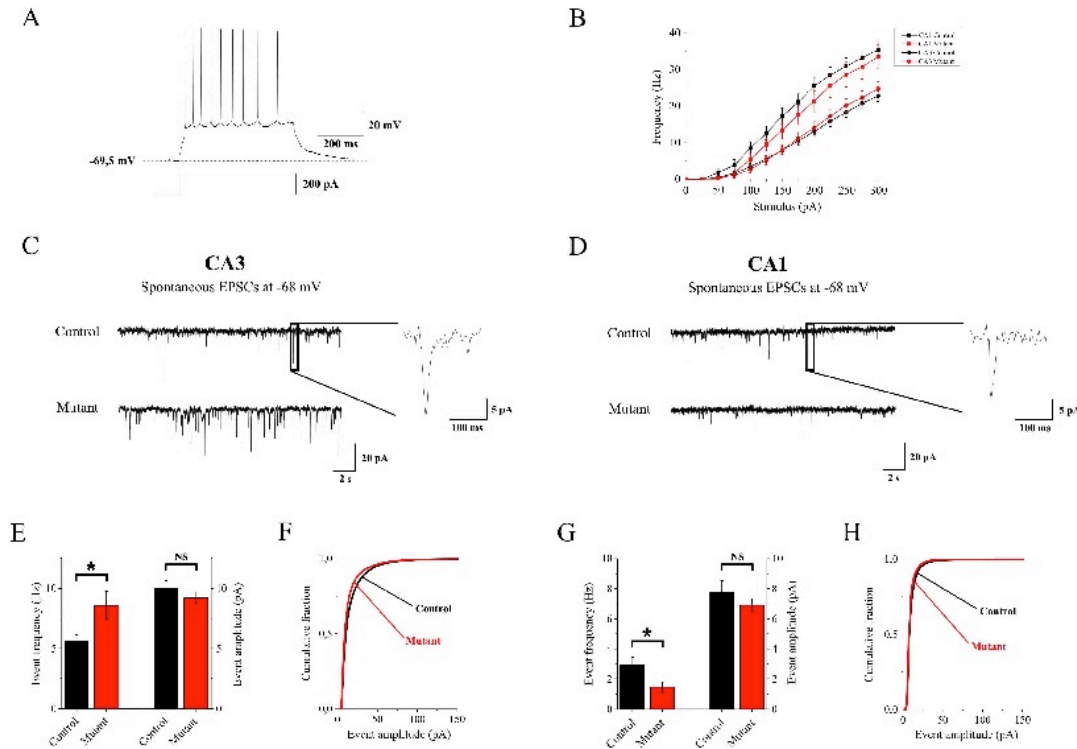
427 Overall, our data indicate significant functional alterations of the hippocampal circuitry in early
428 *Sox2* mutants, which might plausibly contribute to the epileptic and cognitive defects in human
429 patients (see Discussion).

430

431

432

433



434

435

436

Figure 7

437

In *Emx1-Cre cKO* mice, excitatory transmission is altered in CA3 and CA1 hippocampal regions.

438

Early Sox2 ablation leads to alterations in the excitatory input onto both CA3 and CA1 pyramidal neurons.

439

(A) Typical firing response to a 200 pA stimulus of injected current in a CA3 pyramidal neuron. (B) Average

440

stimulus/frequency relation for hippocampal pyramidal neurons recorded in CA3 (Circles) and CA1

441

(Squares). No major differences were observed between control (Black) and mutant animals (Red). (C and

442

D) EPSCs traces, at -68 mV, recorded in simulated physiologic conditions onto pyramidal neurons in CA3

443

and CA1 region respectively. *Insets*. Magnification of a representative EPSC event. (E) Average EPSCs

444

frequencies and median amplitudes observed in CA3 pyramidal neurons recorded from 15 animals between

445

p19 and p31. In mutant animals, Sox2 ablation induced a significant increase in EPSCs frequency compared

446

to controls (8.60 ± 1.15 Hz, $n = 20$ and 5.59 ± 0.57 Hz, $n = 28$ respectively; $p = 0.03941$, with Mann-

447

Whitney test), whereas, no significant effect was produced on event amplitudes (9.21 ± 0.47 pA, $n = 20$ and

448

10.01 ± 0.61 pA, $n = 28$ respectively). (F) Amplitude distribution of the total amount of collected EPSCs

449

showing no major differences between control and mutant mice. (G) In CA1, EPSCs frequency significantly

450

decreased in mutant animals compared to controls (1.46 ± 0.35 Hz, $n = 13$ and 2.91 ± 0.52 Hz, $n = 13$

451

respectively; $p = 0.02745$, with Mann-Whitney test). No difference in the average median amplitude was

452

observed (controls: 7.75 ± 0.69 pA, $n = 20$ and mutants: 6.92 ± 0.44 pA, $n = 28$). (H) The amplitude

453

distribution of the total pool of events recorded from 13 animals between p19 and p31 showed no major

454

alterations between control and mutant mice.

455

456

Discussion

457

458

In this work, we highlighted an early time window in hippocampal development, where the Sox2

459

transcription factor is necessary to initiate the embryogenesis of the hippocampus. In fact, following

460

Sox2 mutation with FoxG1-Cre, active from E8.5 (A. Ferri et al., 2013; Hébert & McConnell,

461 2000), hippocampal development is drastically defective, with a nearly complete absence of the
462 DG; DG development is also defective, but present, following mutation with *Emx1-Cre*, active
463 from E10.5; *Sox2* mutation with *Nestin-Cre* has very little effect on hippocampal embryogenesis
464 (Fig. 2).

465 These observations point to gene regulatory events, orchestrated by *Sox2*, that are required to
466 initiate hippocampal development; at least some of these events are likely to be direct effects of
467 SOX2 (Fig. 6). What is the nature of these events?

468

469 ***Gene regulatory events mediating early Sox2 function in hippocampal development***

470 A severe reduction in the early expression of key regulators of hippocampal development (*Wnt3a*;
471 *Gli3*; *Cxcr4*; *Tbr2*; *p73*) is observed in early *Sox2* mutants (*FoxG1-Cre* cKO), already at early
472 stages of hippocampal embryogenesis (E12.5, E14.5), preceding the overt phenotypic manifestation
473 of the defect (hippocampal morphogenesis begins at about E14.5) (Figs. 4,5). Of note, reduced
474 expression in the mutant CH at E12.5 is seen for some genes (e.g. *Wnt3a*, *Gli3*) but not others
475 (*Wnt5a*; Fig. 5), suggesting that the CH is present, but dysfunctional in directing hippocampal
476 formation. Importantly, a reduction in expression of these master genes is also observed in *Emx1-*
477 *Cre* mutants, but to a lesser extent than in *FoxG1-Cre* mutants (Fig. 5). These observations suggest
478 that the differential reduction in the expression of these key regulators accounts, at least in part, for
479 the differences in the severity of the hippocampal embryogenesis defects between the three mutants.

480

481 What molecular mechanisms cause the differential expression of master hippocampal regulator
482 genes between different mutants?

483 SOX2 is able to directly bind to at least some of these target genes (*Gli3*, *Cxcr4*, Fig. 6A,C) in
484 neural cells chromatin, and to act as a transcriptional activator on some SOX2-bound enhancers
485 (*Gli3*) within these loci (Fig. 6B), suggesting that it is directly involved in the transcriptional
486 activation of at least some of these genes during hippocampal development. Further, SOX2-bound
487 distant enhancers within the *Gli3* and *Cxcr4* loci are connected to the gene promoter in a *Sox2-*
488 dependent way, at least in NSC (Fig. 6A,C), indicating that SOX2 may contribute to their
489 regulation also through this “architectural” function (Bertolini et al., 2019; Wei, Nicolis, Zhu, &
490 Pagin, 2019).

491 At E12.5 and afterwards, *Sox2* is ablated in both *FoxG1-Cre* and *Emx1-Cre* mutants, yet critical
492 genes are much more downregulated in *FoxG1-Cre* mutants, in agreement with a requirement for
493 *Sox2* to properly initiate the expression of these genes at early stages. We speculate that SOX2 may

494 act at early stages to initiate the organization of a 3D interaction network connecting gene
495 promoters to enhancers (Fig. 6A,C), as a prerequisite for gene expression, in agreement with
496 previous findings in NSC (Bertolini et al., 2019; Wei et al., 2019).

497

498 ***Altered regulation of a gene regulatory network of hippocampal master genes leads to defective***
499 ***cell development and cell-cell signaling in early Sox2 mutants, and eventually to defective***
500 ***hippocampal structure and function***

501 The failure to properly activate early-acting hippocampal master genes may provide a molecular
502 explanation to the failure to develop, in early Sox2 mutants, cell types essential in hippocampal
503 development, or to prevent their proper behavior, as observed in Figs. 2,3.

504

505 In FoxG1-Cre, but not in Emx1-Cre Sox2 mutants, the Gli3 gene is downregulated at early stages
506 (E12.5) in the segment of medial telencephalic wall required for hippocampal development, the CH
507 (Fig. 5H,I). Gli3 encodes a transcription factor, and its homozygous mutation (as in the *extra-toes*
508 Gli3^{Xt/Xt} mouse mutant) leads to absence of the hippocampus (Li & Pleasure, 2014; Theil, Alvarez-
509 Bolado, Walter, & Ruther, 1999). In Gli3 mutant embryos, the medial wall of the telencephalon
510 fails to invaginate to initiate hippocampal development, pointing to an early defect of the
511 proliferating neuroepithelial cells of the prospective hippocampus (Li & Pleasure, 2014; Theil et al.,
512 1999). Mutations of human GLI3 cause Pallister-Hall syndrome and Greig cephalopolysyndactyly
513 syndrome, a complex defect that can involve seizures and intellectual disability, though
514 hippocampal abnormalities were not specifically investigated (Naruse, Ueta, Sumino, Ogawa, &
515 Ishikiriya, 2010). In mouse Gli3 mutants, the expression of Wnt signaling molecules, normally
516 expressed in the CH, including Wnt3a and Wnt2b, is lost, and Wnt signaling is impaired at early
517 stages of hippocampal development (Fotaki, Price, & Mason, 2011; Grove et al., 1998; Theil,
518 Aydin, Koch, Grotewold, & Ruther, 2002).

519

520 The expression of Wnt3a and Wnt2b, encoding secreted signaling molecules produced by the CH
521 signaling center, is also defective in early Sox2 mutants (Fig. 5); their downregulation is most
522 pronounced in FoxG1-Cre mutants, less so in Emx1-Cre mutants (see above and Fig. 5A,B,D,E).
523 The downregulation of Gli3 may contribute to this (see above).

524

525 Wnt signaling exerts its effects on target cells by inducing nuclear translocation of beta-catenin, that
526 acts as a transcriptional regulator associating with TCF transcription factors; mutation of TCF

527 factors, e.g. Lef1, leads to failure of hippocampal development (Galceran, Miyashita-Lin, Devaney,
528 Rubenstein, & Grosschedl, 2000; Li & Pleasure, 2014; Roelink, 2000). Of note, TCF binding
529 regulates (Hasenpusch-Theil et al., 2012) the same intronic Gli3 enhancer, that we found to be
530 bound and activated by Sox2 (Fig. 6A,B), suggesting that this element may integrate the effects of
531 Wnt signaling and SOX2 activity in controlling Gli3 expression. Interestingly, Sox2/TCF binding
532 sites were also described to act on other genes in the context of a transcriptional switch
533 accompanying chromatin remodeling during neuronal differentiation (Muotri et al., 2010).

534

535 We attempted to reactivate the Wnt pathway in the FoxG1-Cre cKO, by LiCl injection, to see if we
536 could rescue any of the observed defects. We found some amelioration of the organization and
537 number of CRC in the cortex (Fig. S3B,C), although the overall hippocampus development
538 remained defective (Fig. S3A,C). We also tried to reactivate the Wnt pathway by a Wnt agonist
539 (AZD 1080); a partial rescue of Reelin retention in the CH, usually observed in mutants, was
540 observed at E14.5 in the FoxG1-Cre cKO (Fig. S3D). We hypothesized that earlier treatment might
541 have had more pronounced effects, however this resulted in high embryonic lethality, preventing us
542 to observe the effects.

543 In conclusion, we propose that loss of Wnt signaling from the CH represents one mechanism
544 whereby Sox2 early loss causes defective hippocampal embryogenesis likely by regulating the
545 production of CRC. Assessing the relative contribution of this mechanism will be postponed to
546 future studies.

547

548 We detected, in our early mutants, reduced expression of Tbr2, Cxcr4, Cxcl12 and p73, marking
549 specific cell types in hippocampal embryogenesis (Fig. 4). However, knock-out experiments
550 previously demonstrated that these genes, further to marking specific cell types (see Fig. 2), also
551 play functional roles in hippocampal (as well as neocortical) development (Bagri et al., 2002;
552 Hodge et al., 2013; Lu, Grove, & Miller, 2002; Meyer et al., 2004; Mimura-Yamamoto et al.,
553 2017). This suggests that their reduced expression in Sox2 mutants may also functionally contribute
554 to the hippocampal defects.

555 Cxcr4, whose expression is downregulated at early stages in Sox2 early mutants (Fig. 4G), is
556 essential in particular for the development of the DG (Lu et al., 2002; Mimura-Yamamoto et al.,
557 2017). Cxcr4 encodes a cell surface receptor, expressed in Granule Cell Progenitors (GCP) of the
558 developing hippocampus, that also express GFAP (Mimura-Yamamoto et al., 2017). In
559 hippocampal development, GCP, arising in the ventricular zone (DNE), migrate (dentate migratory

560 stream) to the subpial region, to form the granule cell layer (GCL) of the DG (Fig. 1A). The
561 production and migration of GCP is regulated by various signaling molecules, including CXCL12
562 (the CXCR4 ligand), Reelin, Wnt, and BMP proteins, secreted by regions surrounding the
563 developing DG. In the absence of Cxcr4, the numbers of dividing cells in the migratory stream and
564 the prospective DG is dramatically reduced (Lu et al., 2002). It thus seems plausible that Cxcr4
565 deficiency importantly contributes to the impaired development of GFAP-positive GCP, and the
566 consequent failure to develop a DG, seen in our early Sox2 mutants.

567 P73 encodes a transcription factor expressed in differentiating CRC (Fig. 4), the choroid plexus and
568 the ependyma (Meyer, Schaaps, Moreau, & Goffinet, 2000; Yang et al., 2000) and its knock-out in
569 mice results in a phenotype very similar to the early loss of Sox2 in FoxG1-Cre cKO, with a lack of
570 HF and almost absent DG (Meyer et al., 2019). P73 has a similar expression pattern in the fetal
571 human brain suggesting a role in hippocampus development also in humans (Meyer et al., 2019).
572 Interestingly, Reelin-expressing CRC in Sox2 mutants are similarly reduced in number and they
573 may be retained in the cortical hem instead of moving towards the pia. P73 has a very restricted
574 expression pattern, but its knock-out has a broad effect on cortical patterning suggesting it could be
575 involved in the signaling activities of the CH (Meyer et al., 2004).

576

577 ***Radial scaffold, Cajal-retzius cells and lack of hippocampal fissure and dentate gyrus***

578 One of the key outcomes of early ablation of Sox2 in the developing telencephalon, via FoxG1-Cre,
579 is the lack of the hippocampal fissure followed by an extreme reduction of the DG. Radial glia
580 scaffold disorganization due to knock-out of the transcription factor Nflb leads to lack of a specific
581 hippocampal GFAP-positive glial population, lack of hippocampal fissure and DG without
582 affecting cell proliferation, CRC differentiation or Wnt signalling (Barry et al., 2008); this suggests
583 that the loss and disorganization of GFAP-positive cells, seen in our mutants specifically in the
584 developing hippocampus (Fig. 3), might constitute a cellular mechanism contributing to the
585 defective DG development in early Sox2 mutants.

586 Knock-out of P73 in CH-derived CRC cells leads to lack of hippocampal fissure and DG, as
587 previously mentioned (Meyer et al., 2004). CRC are known to regulate RG formation both in the
588 cortex and in the developing hippocampus (Forster et al., 2002; Frotscher, Haas, & Forster, 2003);
589 conversely, RG has been shown to be important for the correct positioning of CRC cells (Kwon,
590 Ma, & Huang, 2011). Our data suggests that Sox2 does not regulate proliferation in the medial
591 telencephalon at E12.5 (Fig. S2); it is possible that it regulates aspects of differentiation of RG and
592 CRC.

593

594 ***Functional alteration of hippocampal circuitry in Sox2-ablated mice***

595 In Emx1-Cre Sox2-deleted mice, we observed functional alterations in the excitatory transmission
596 along the serial transmission pathway of the hippocampal formation, and particularly an imbalance
597 in the excitatory input onto CA3 and CA1 pyramidal neurons (Fig. 7). Considering that i) the main
598 effects of Sox2 ablation are produced during hippocampal embryogenesis, ii) Sox2 is not expressed
599 in CA3/CA1 neurons, iii) Sox2 deletion caused negligible alterations in pyramidal neuron
600 excitability and excitatory synaptic efficacy, we attribute most of the observed functional effects to
601 altered maturation of the connectivity pattern of hippocampal formation. Neural circuits in the
602 hippocampal formation comprise both serial and parallel pathways. DG is regulated by cortical
603 input from entorhinal layer III, and projects to CA3. However, entorhinal layer III also projects to
604 CA3. Moreover, CA3 displays profuse recurrent reciprocal connections between pyramidal neurons
605 (Witter & Amaral, 2004). Therefore, the higher EPSC frequency we observed in CA3 pyramidal
606 neurons of Sox2-deleted mice could be caused by: i) a denser innervation from entorhinal layer III,
607 permitted by the lower entorhinal input to the hypoplastic DG; ii) an increased recurrent collateral
608 connectivity between CA3 cells, fostered by the absence of the physiological stimulus from DG; iii)
609 a decreased recurrent inhibition on CA3 pyramidal cells, as mossy fibers from DG also regulate
610 GABAergic interneurons in CA3 (Acsady, Kamondi, Sik, Freund, & Buzsaki, 1998). We cannot
611 presently distinguish between these mechanisms, which are not mutually exclusive. Nonetheless,
612 the increased excitatory input we observed in CA3 pyramidal cells is consistent with the epileptic
613 phenotype frequently associated with the brain malformations caused by Sox2 mutations (Sisodiya
614 et al., 2006). Considering the peculiar propensity of CA3 region to develop seizure-like activity (de
615 la Prida, Huberfeld, Cohen, & Miles, 2006; Miles & Wong, 1983), we hypothesize that increased
616 excitatory activity in CA3 of Sox2-deleted mice could facilitate seizure onset, perhaps through CA3
617 projection to septal areas (Colom, 2006; Swanson & Cowan, 1977).

618 By contrast, the excitatory input on CA1 pyramidal neurons was lower in Emx1-Cre cKO mice.
619 This could be caused by increased local feed-back inhibition by GABAergic neurons, because of
620 overstimulation by the overactive CA3 fibers. Alternatively, in the absence of proper DG input, the
621 partial disorganization of CA3 connectivity could favor recurrent collaterals at the expense of
622 Schaffer collaterals. Regardless of the specific mechanism, our results demonstrate that Sox2
623 ablation at early developmental stages unbalances the normal CA3 to CA1 excitatory input, which
624 could contribute to explain some of the cognitive alterations observed in Sox2 mutants. Although
625 early Sox2 ablation leads to severe DG hypoplasia, many cognitive functions can be carried out

626 even when hippocampal volume is strongly reduced (Moser & Moser, 1998; Sisodiya et al., 2006).
627 It is therefore not surprising that the effects of Sox2 ablation on cognition of viable animals are
628 subtle. Nonetheless, evidence is available in humans about a variety of cognitive alterations
629 associated with Sox2 mutations (Ragge et al., 2005; Sisodiya et al., 2006). In general, CA1 is the
630 main output channel of the hippocampal formation, and is thought to compare the entorhinal cortex
631 input (conveying the present state of the environment) with the CA3 input (conveying mnemonic
632 representations of expected events based on external signals; (Knierim & Neunuebel, 2016). Our
633 results suggest that Sox2 malfunction may cause cognitive damage by altering such comparative
634 function of CA1.

635

636 ***Conclusion and perspective***

637 Overall, our work shows that Sox2 controls (directly, or indirectly) the activity of multiple,
638 functionally interconnected genes, forming a gene regulatory program active and required at very
639 early stages of hippocampal development. Reduced activity of this program leads to essentially
640 absent (FoxG1-Cre mutants) or reduced (Emx1-Cre mutants) development of the hippocampus, in
641 particular the DG. In the Emx1 mutants, which are viable, hippocampal physiology is importantly
642 perturbed. These findings may provide novel perspectives for therapy approaches of genetic brain
643 disease rooted in defective hippocampal development.

644

645

646 **Materials and methods**

647

648 *Mouse strains*

649 Mutant mice were obtained by crossing the Sox2Flox (Favaro et al., 2009) line with the following
650 lines: FoxG1-Cre (Hébert & McConnell, 2000), Emx1-Cre (Gorski et al., 2002) and Nestin-Cre;
651 Sox2 β Geo (Tronche et al., 1999); Medina, 2004 #506; Favaro, 2009 #3}. The mouse line Sox2-
652 CreERT2 (Favaro et al., 2009), was crossed to a transgenic mouse line with a *loxP-EYFP* reporter
653 of Cre activity (Rosa26R-EYFP) (Srinivas et al., 2001) to determine the progeny of Sox2
654 expressing cells following tamoxifen injection (as described below).

655 The day of vaginal plug was defined as embryonic day 0 (E0) and the day of birth as postnatal day
656 0 (P0).

657 Genotyping of adult mice or embryos was performed with the following primers:

658 Sox2 Flox Forward: 5' AAGGTACTGGGAAGGGACATTT 3'

659 Sox2 Flox Reverse: 5'AGGCTGAGTCGGGTCAATTA 3'
660 FoxG1-Cre Forward: 5' AGTATTGTTTTGCCAAGTTCTAAT 3'
661 FoxG1-Cre Reverse: 5'AGTATTGTTTTGCCAAGTTCTAAT 3'
662 Emx1-Cre IRES Forward: 5'AGGAATGCAAGGTCTGTTGAAT 3'
663 Emx1-Cre IRES Reverse: 5' TTTTCAAAGGAAAACCACGTC 3'
664 Nestin-Cre Forward: 5' CGCTTCCGCTGGGTCACTGTCG 3'
665 Nestin-Cre Reverse: 5' TCGTTGCATCGACCGGTAATGCAGGC 3'
666 R26R-EYFP Forward: 5' TTCCCGCACTAACCTAATGG 3'
667 R26R-EYFP Reverse: 5' GAACTTCAGGGTCAGCTTGC 3'
668 Sox2-CreERT2 Forward: 5' TGATCCTACCAGACCCTTCAGT 3'
669 Sox2-CreERT2 Reverse: 5' TCTACACATTTCCCTGGTTC 3'

670 The FoxG1-Cre mouse line was maintained in 129 background as recommended in (Hébert &
671 McConnell, 2000). The other mouse lines were maintained in a mixed background enriched in
672 C57BL/6 and DBA.

673 All procedures were in accordance with the European Communities Council Directive (2010/63/EU
674 and 86/609/EEC), the National Institutes of Health guidelines, and the Italian Law for Care and Use
675 of Experimental Animals (DL26/14). They were approved by the Italian Ministry of Health and the
676 Bioethical Committees of the University of Milan-Bicocca.

677

678

679 *In situ hybridization*

680 *In situ* hybridization was performed essentially as in (Mercurio et al., 2019). Briefly, embryonic
681 brains and P0 brains were dissected and fixed overnight (O/N) in paraformaldehyde 4% in PBS
682 (Phosphate Buffered Saline; PFA 4%) at 4°C. The fixed tissue was cryoprotected in a series of
683 sucrose solutions in PBS (15%, 30%) and then embedded in OCT (Killik, Bio-Optica) and stored at
684 -80°C. Brains were sectioned (20 µm) with a cryostat, placed on a slide (Super Frost Plus 09-
685 OPLUS, Menzel) and stored at -80°C. Slides were then defrosted, fixed in formaldehyde 4% in
686 PBS for 10 minutes (min), washed 3 times for 5 min in PBS, incubated for 10 min in acetylation
687 solution (for 200 ml: 2.66 ml triethanolamine, 0.32 ml HCl 37%, 0.5 ml acetic anhydride 98%) with
688 constant stirring and then washed 3 times for 5 min in PBS. Slides were placed in a humid chamber
689 and covered with prehybridization solution (50% formamide, 5X SSC, 0.25 mg/ml tRNA, 5X
690 Denhardt's, 0.5 µg/ml salmon sperm) for at least 2 hours (h) and then incubated in hybridization
691 solution (fresh prehybridization solution containing the digoxigenin (DIG)-labelled RNA probe of

692 interest) O/N at 65°C. Slides were washed 5 min in 5X SSC, incubated 2 times in 0.2X SSC for 30
693 min at 65°C, washed 5 min in 0.2X SSC at room temperature (RT) and then 5 min in Maleic Acid
694 Buffer (MAB, 100 mM maleic acid, 150 mM NaCl pH 7.5). The slides were incubated in blocking
695 solution (10% sheep serum, 2% blocking reagent (Roche), 0.3% Tween-20 in MAB) for at least 1 h
696 at RT, then covered with fresh blocking solution containing anti-DIG antibody Roche © 1:2000 and
697 finally placed O/N at 4°C. Slides were washed in MAB 3 times for 5 min, in NTMT solution (100
698 mM NaCl, 100 mM Tris-HCl pH 9.5, 50 mM MgCl₂, 0.1% Tween-20) 2 times for 10 min and then
699 placed in a humid chamber, covered with BM Purple (Roche), incubated at 37°C until desired
700 staining was obtained (1-6 h), washed in water for 5 min, air dried and mounted with Eukitt
701 (Sigma).

702 The following DIG-labelled probes were used: *Sox2* (Avilion et al., 2003), *Cadherin8* (Korematsu
703 & Redies, 1997), *Tbr2* (Bulfone et al., 1999), *Reelin* (a gift from Luca Muzio, HSR Milan), *Cxcr4*
704 (Lu et al., 2002), *Cxcl12* (Lu et al., 2002), *Wnt3A* (Grove et al., 1998), *Wnt2b* (Grove et al., 1998),
705 *Wnt5a* (Grove et al., 1998), *Gli3* (a gift from Luca Muzio, HSR Milan), *Lhx2* (a gift from Shubha
706 Tole, Tata Institute Mumbai), *P73* (a gift from Olivia Hanley, UZH). The *P73* probe was
707 transcribed directly from a PCR product, obtained from E12.5 cDNA, with the following primers:
708 Forward 5' AGCAGCAGCTCCTACAGAGG 5' and Reverse 5'
709 TAATACGACTCACTATAGGGCCTTGGGAAGTGAAGCACTC 3' (which includes the T7
710 promoter underlined).

711

712 *Immunohistochemistry*

713 Immunohistochemistry was performed essentially as in (Cerrato et al., 2018). Brains were
714 dissected, fixed, embedded and sectioned as for *in situ* hybridization, except for fixation in PFA4%
715 that was often 3-4h at 4°C. Sections were washed in PBS 5 min, unmasked in citrate buffer (Na
716 Citrate 0.01M, Citric acid 0.01M pH6) by boiling in a microwave 3 min and then washed in PBS 10
717 min at RT. Sections were blocked with blocking solution (FBS 10%, Triton 0.3%, PBS1X) for 1h at
718 RT, then incubated O/N in blocking solution with primary antibodies: anti-mSOX2 (R&D Systems
719 MA2018, 1:50), anti-P73 (Neomarkers, 1:150), anti-Reelin (Millipore MAB5364, 1:500), anti-Tuj1
720 (Covance, 1:400), anti-GFP (Invitrogen A10262, 1:500, used to detect EYFP expressing cells), anti-
721 GFAP (Dako, 1:500). Slides were then washed in PBS 2 times, 10 min each, and incubated in
722 blocking solution containing the secondary fluorescent antibody (1:1000, Alexa Fluor Invitrogen)
723 for 1h 30 minutes at RT. Slides were then washed in PBS twice, 10 minutes each, and then mounted
724 with Fluormount (F4680, Sigma) with 4',6-diamidino-2-phenylindole (DAPI) and imaged with a

725 confocal microscope (Nikon A1R) and with a Zeiss Axioplan 2 Fluorescent microscope for anti-
726 GFAP immunostainings.

727

728 *Lineage tracing of progeny of Sox2 expressing progenitors*

729 R26R-EYFP females were crossed with Sox2-CreERT2 males. E9.5 pregnant females were injected
730 intraperitoneally with tamoxifen (20 mg ml⁻¹ in ethanol/corn oil 1:10, 0.1 mg per g of body weight)
731 that induces Cre recombinase activity in the Sox2 telencephalic expression domain (Favaro et al.,
732 2009) and therefore turns on EYFP in this expression domain. Embryos were collected at E15.5,
733 fixed in 4% PFA O/N, embedded in OCT and sectioned at the cryostat (20- μ m sections) as for *in*
734 *situ* hybridization (see above).

735 *EdU tracing*

736 Ethynyldeoxyuridine (EdU, Molecular Probes) was injected in E12.5 pregnant females at 50 μ g/g
737 body weight. Embryos were collected 30 min after injection, fixed O/N in PFA 4% and embedded
738 for cryostat sectioning as above. Edu incorporation was detected on sections (20 μ m) with the
739 Click-iT EdU Kit Alexa Fluor 594 (C10354, Thermo Fisher) following manufacturer's instructions.
740 Briefly, slides were washed twice in PBS 2 min each and incubated for 20 min at RT in Triton 0.5%
741 in PBS. Slides were then washed in Triton 0.1% in PBS 3 times, 3 min each. Sections were
742 incubated 30 min in the dark with EdU Click reaction according to manufacturer's instructions.
743 Slides were then washed in PBS 3 times 5 min, stained with DAPI, mounted with Fluoromount
744 (F4680, Sigma) and imaged with a confocal microscope (Nikon A1R). The number of EdU positive
745 cells in the cortical hem and dentate neuroepithelium was counted on at least 3 consecutive coronal
746 sections for each brain. Data are represented as mean \pm standard deviation.

747

748 *Brain slices*

749 For patch-clamp experiments, coronal sections (300 μ m thick) containing the hippocampal region (-
750 1.22 mm to -2.70 mm from bregma) were prepared from mice of both sexes (6M and 10F) aged P19-
751 P31, by applying standard procedures (Aracri, Meneghini, Coatti, Amadeo, & Becchetti, 2017).

752

753 *Patch-clamp recording and data analysis*

754 Cells were examined with an Eclipse E600FN direct microscope, equipped with water immersion
755 DIC objective (Nikon Instruments, Milano, Italy), and digital CCD C8484-05G01 IR camera with
756 HCImage Live acquisition software (Hamamatsu Photonics Italia, Arese, Italy). Stimulation and
757 recording were carried out in whole-cell mode, by using a Multiclamp 700A amplifier (Molecular
758 Devices, Sunnyvale, CA), at 33-34°C. Borosilicate capillaries (OD 1.5 mm; Corning Inc., NY) were
759 pulled (2-3 M Ω) with a Flaming/Brown P-97 micropipette puller (Sutter Instruments, Novato, CA).
760 Series resistance after patch rupture was usually around 10-15 M Ω and was compensated up to at
761 least 70%. Cell capacitance was also compensated. Synaptic currents and action potentials were low-
762 pass filtered a 2 kHz e digitized at 5 kHz with Digidata 1322A / pClamp 9.2 (Molecular Devices).
763 During recording, slices were perfused (~2 ml/min) with artificial cerebrospinal fluid, containing
764 (mM): 135 NaCl, 21 NaHCO₃, 0.6 CaCl₂, 3 KCl, 1.25 NaH₂PO₄, 1.8 MgSO₄, 10 D-glucose, aerated
765 with 95% O₂ and 5% CO₂ (pH 7.4). Pipette contained (mM): 140 K-gluconate, 5 KCl, 1 MgCl₂, 0.5
766 BAPTA, 1 MgATP, 0.3 NaGTP, 10 HEPES (pH 7.26). Resting membrane potential (V_{rest}) was
767 determined in open circuit mode ($I=0$), immediately after reaching the whole-cell configuration. No
768 correction was applied for liquid junction potentials. Series resistance was monitored throughout the
769 experiment by applying small stimuli around V_{rest} . Cells were discarded when R_s was higher than 15
770 M Ω .

771 Action potentials and EPSCs were analysed with Clampfit 9.2 (Molecular Devices), MiniAnalysis,
772 and OriginPro 9.1(OriginLab Corporation, Northampton, MA, USA), as previously reported
773 (Aracri, Amadeo, Pasini, Fascio, & Becchetti, 2013; Aracri et al., 2017).

774
775

776 *AZD and LiCl treatment*

777 AZD 1080 (Axon Medchem, Axon Catalog ID: 2171) diluted in ascorbic acid 0.5%/EDTA 0.01%,
778 was administered to pregnant females once a day by oral gavage from E9.5 to E12.5. We
779 administered 5 μ l AZD/g of body weight (AZD 0.375 μ g/ μ l at E9.5 and E10.5, AZD 0.75 μ g/ μ l at
780 E11.5 and E12.5). Embryos were then collected at E14.5. Ascorbic acid 0.5%/EDTA 0.01% was
781 administered as a control.

782 LiCl, or NaCl as a control, were injected intraperitoneally in pregnant female from E9.5 to E14.5 or
783 from E10.5 to E12.5 once a day at the same time. No difference was observed between the two
784 injection time windows. 10 μ l/ g of body weight of 600 mM LiCl or 600 mM NaCl were injected.
785 Embryos were collected at E18.5 and processed for *in situ* hybridization. Injection of AZD 1080 or
786 LiCl in pregnant females at E8.5 led to abortions.

787 The number of *Reelin*-positive cells at the hippocampal fissure and in the cortex was counted using
788 Photoshop CC 2015 on five consecutive coronal sections of each brain. Data are represented as
789 mean \pm standard deviation and were statistically analyzed using unpaired Student's T-test,
790 *** $p < 0.005$.

791

792 *Luciferase constructs*

793 The DNA region in the Gli3 second intron overlapping the SOX2 peak, and corresponding to the
794 VISTA enhancer (coordinates under the embryo in Fig. 6A) was PCR-amplified from the vector
795 where it had been cloned upstream to the lacZ reporter (a gift from T. Theil; (Hasenpusch-Theil et
796 al., 2012)), and cloned upstream to the tk promoter in the Tk-luc vector (Mariani et al., 2012), into
797 the KpnI and NheI restriction sites.

798

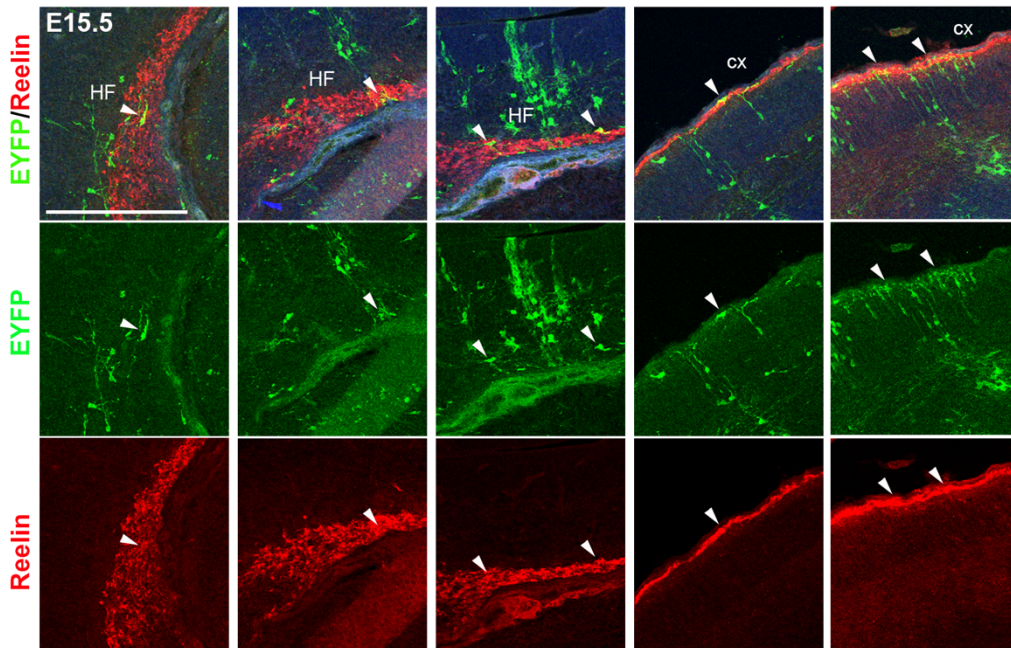
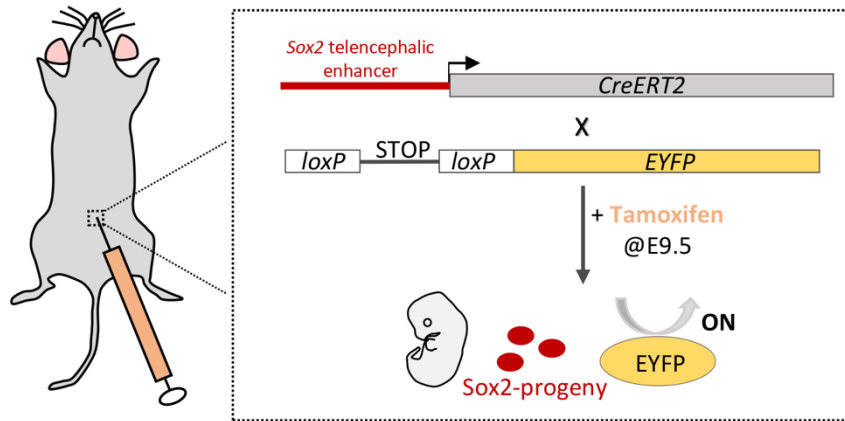
799 *Transfection experiments*

800 The transfection experiments were performed essentially as previously described (Mercurio et al.,
801 2019; Panaliappan et al., 2018). In particular, Neuro-2a cells were plated in Minimal Essential
802 Medium Eagle (MEM; SIGMA), supplemented with 10% Foetal Bovine Serum, L-Glutamine,
803 penicillin and streptomycin. For transfection, cells were plated in 12-well plates at 1.5×10^5
804 cells/well, and transfected on the following day using Lipofectamine 2000 (Invitrogen). Briefly,
805 medium in each well was replaced with 1 ml of MEM medium (with no addition) mixed with 2 μ l
806 of Lipofectamine 2000, and DNA. After 4 hours from transfection, the medium was replaced with
807 complete medium. A fixed amount of 300 ng of luciferase reporter plasmid was used for each well,
808 with increasing amounts of Sox2 expressing vector (Favaro et al., 2009; Mariani et al., 2012), or the
809 corresponding control "empty" vector (not containing the transcription factor's cDNA), in the
810 following luciferase vector:expressing vector molar ratios (indicated in Fig.6): +, 1:0.050; ++,
811 1:0.075; +++, 1:0.125; +++, 1:0.25; +++++, 1:0.5. The pBluescript vector was added to
812 transfection DNA to equalize the total amount of transfected DNA to a total of 800 ng for each
813 reaction. After 24 hours, total cellular extracts were prepared, and Luciferase activity was measured
814 with a Promega Luciferase Assay System, according to the manufacturer's instructions.

815

816

817



818

819 **Supplementary Figure 1**

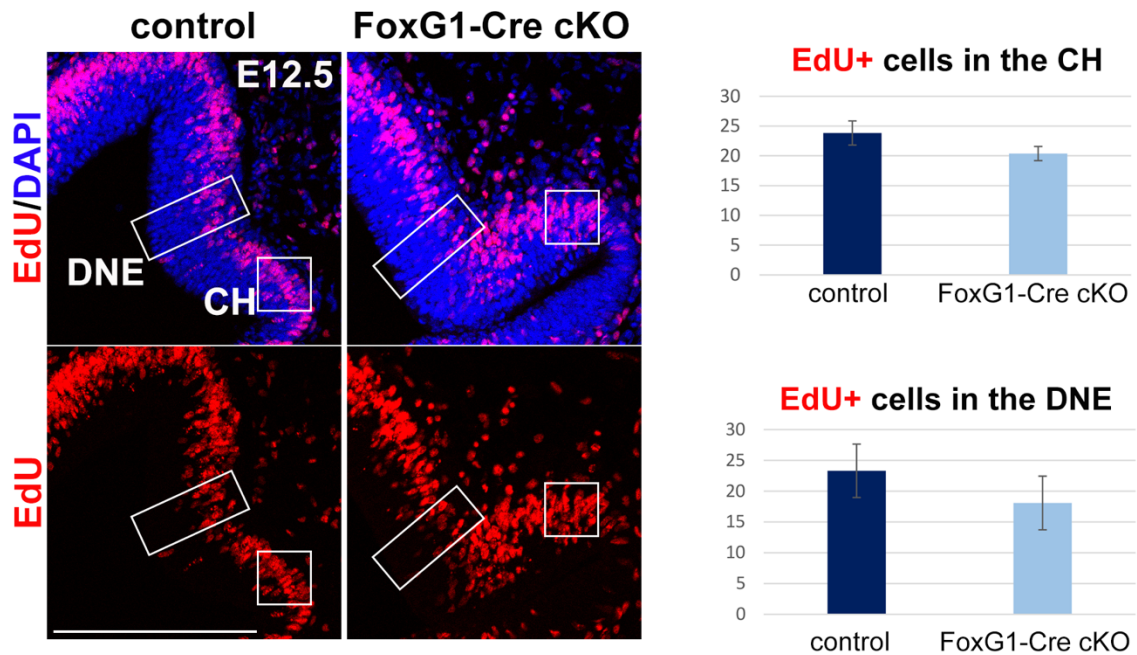
820 **Lineage tracing of Sox2 expressing progeny in CR cells in the hippocampal fissure (HF) and the**

821 **cortex.**

822 Top, scheme depicting the mouse crosses used to trace the progeny of Sox2 expressing cells. A mouse in
823 which expression of an inducible Cre recombinase (cre-ERT2) was under the control of a Sox2 telencephalic
824 enhancer was crossed to a mouse in which YFP expression would be turned on when Cre recombinase was
825 expressed, following tamoxifen injection.

826 Bottom, immunofluorescence for GFP (green) and Reelin (red) on coronal sections of brains at E15.5 from
827 pregnant females injected with tamoxifen at E9.5. Arrows indicate cells that are positive for both GFP and
828 Reelin in the hippocampal fissure (HF) and the cortex (cx). Scale bar 200 μ m.

829



830

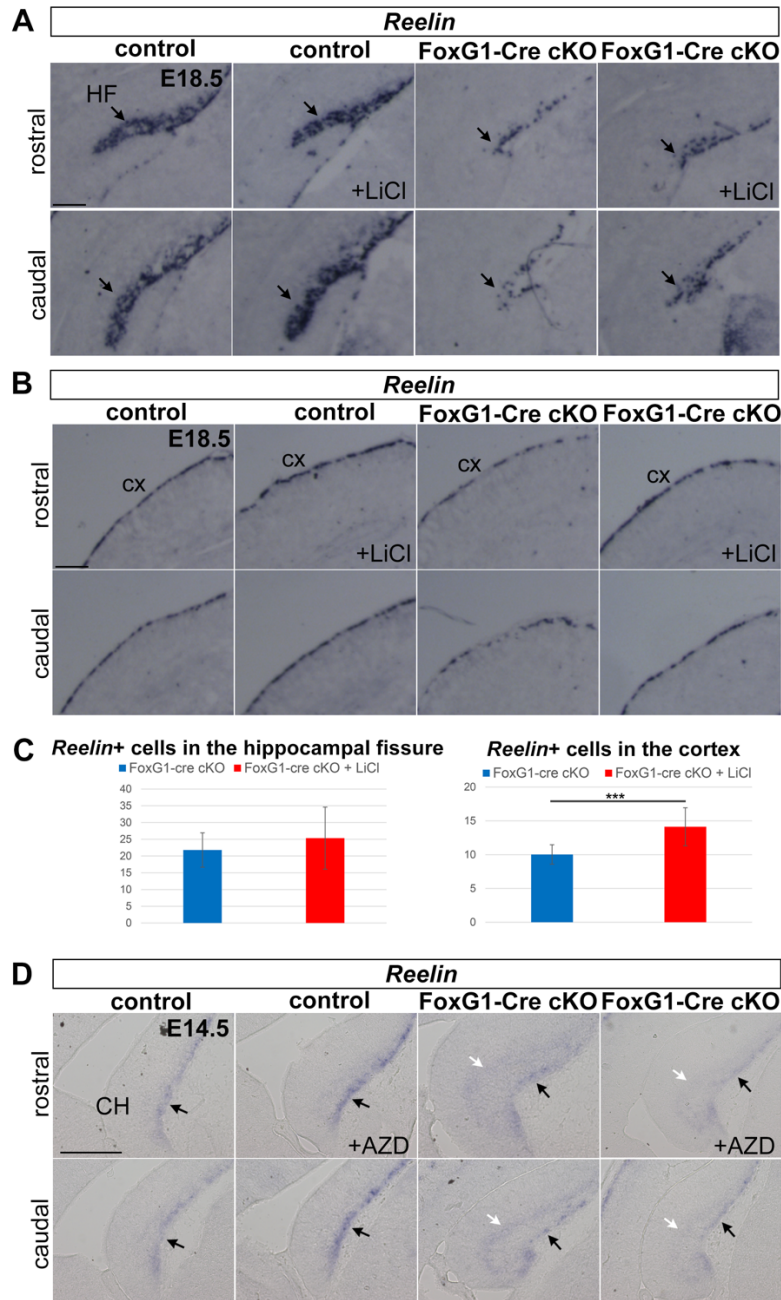
831 **Supplementary Figure 2**

832 **Sox2 early ablation does not appear to affect cellular proliferation neither in the**
833 **cortical hem nor in the dentate neuroepithelium**

834 EdU staining on coronal sections of control and FoxG1-Cre cKO mice at E12.5 injected with EdU
835 and sacrificed 30 minutes later. The graphs on the right show no significant difference in the
836 number of proliferating cells in the cortical hem (CH) and in the dentate neuroepithelium (DNE) at
837 the developmental stage analysed. Data are represented as mean \pm standard deviation (controls n=3,
838 mutants n=3). Scale bar 200 μ m.

839

840



841

842 **Supplementary Figure 3**

843 **Administration of agonists of the Wnt pathway LiCl and AZD 1080 partially rescues the deficit of C-R**
844 **cells in the cortex, but only slightly in the hippocampal fissure.**

845 *Reelin in situ* hybridization on coronal sections of control or FoxG1-Cre cKO brains injected with Wnt
846 agonists, at the times indicated, and analyzed at E18.5 in the case of LiCl injection (**A,B**) and at E14.5 for
847 AZD 1080 injection (**D**). LiCl or NaCl were intraperitoneally injected once a day in pregnant females from
848 E10.5 to E12.5. AZD 1080 was administered by oral gavage once a day in pregnant females from E9.5 to
849 E12.5. At least 3 controls and 3 mutants, both treated and untreated, were analyzed. The graphs in (**C**)
850 indicate a significant rescue in the number of C-R cells in the cortex following LiCl injection (***) $p < 0.005$,
851 unpaired Student's T-test. Mutants untreated $n=5$, mutants LiCl treated $n=5$). Error bars represent standard
852 deviation. (**D**) Black arrows indicate Reelin expressing cells towards the pial side of the cortical hem, white
853 arrows indicate Reelin expressing cells retained in the cortical hem that did not move towards the pia. AZD
854 1080 treatment rescued this retention. Scale bars 200 μm .

855 **Excitability features of CA1/CA3 pyramidal neurons of Emx1-Cre cKO and control mice.**

856

857

Genotype	V_{rest} (mV)	Rheobase (pA)	1 st spike width (ms)	2 nd spike width (ms)	AHP (mV)	1 st to 2 nd spike interval (ms)	4 th to 5 th spike interval (ms)
CA1							
WT	-69.0 ±0.47	92.7 ±6.6	1.22 ±0.04	1.29 ±0.04	-4.16 ±0.6	25.2 ±3.0	42.8 ±3.8
Emx1-Cre cKO	-69.1 ±0.23	100.0 ±5.7	1.26 ±0.05	1.32 ±0.05	-5.11 ±1.2	34.2 ±3.9	59.4 ±6.0
CA3							
WT	-69.7 ±0.23	100.0 ±5.9	1.09 ±0.02	1.17 ±0.02	-5.7 ±0.4	39.4 ±4.3	73.9 ±6.7
Emx1-Cre KO	-69.8 ±0.18	110.0 ±6.4	1.16 ±0.04	1.24 ±0.04	-5.4 ±0.5	36.2 ±1.9	73.7 ±5.8

858

859

860

861 **Supplementary Table 1**

862 **Excitability features of CA1/CA3 pyramidal neurons of Emx1-Cre cKO and control mice.**

863 For the WT and Emx1-Cre cKO mice, the main excitability features are given for CA3 and CA1 pyramidal
 864 neurons, as indicated. The table reports average V_{rest} , rheobase, spike widths (measured at half-amplitude) of
 865 the first and second action potential, and AHP amplitude (with respect to V_{rest}). As a measure of firing
 866 adaptation, the time intervals are reported between the first and second spike and the fourth and fifth spike.

867

868

869 **References**

870

- 871 Acsady, L., Kamondi, A., Sik, A., Freund, T., & Buzsaki, G. (1998). GABAergic cells are the major
872 postsynaptic targets of mossy fibers in the rat hippocampus. *The Journal of neuroscience :
873 the official journal of the Society for Neuroscience*, *18*(9), 3386-3403. Retrieved from
874 <https://www.ncbi.nlm.nih.gov/pubmed/9547246>
- 875 Aracri, P., Amadeo, A., Pasini, M. E., Fascio, U., & Becchetti, A. (2013). Regulation of glutamate
876 release by heteromeric nicotinic receptors in layer V of the secondary motor region (Fr2) in
877 the dorsomedial shoulder of prefrontal cortex in mouse. *Synapse*, *67*(6), 338-357.
878 doi:10.1002/syn.21655
- 879 Aracri, P., Meneghini, S., Coatti, A., Amadeo, A., & Becchetti, A. (2017). alpha4beta2(*) nicotinic
880 receptors stimulate GABA release onto fast-spiking cells in layer V of mouse prefrontal
881 (Fr2) cortex. *Neuroscience*, *340*, 48-61. doi:10.1016/j.neuroscience.2016.10.045
- 882 Avilion, A. A., Nicolis, S. K., Pevny, L. H., Perez, L., Vivian, N., & Lovell-Badge, R. (2003). Multipotent
883 cell lineages in early mouse development depend on SOX2 function. *Genes & development*,
884 *17*(1), 126-140. doi:10.1101/gad.224503
- 885 Bagri, A., Gurney, T., He, X., Zou, Y. R., Littman, D. R., Tessier-Lavigne, M., & Pleasure, S. J. (2002).
886 The chemokine SDF1 regulates migration of dentate granule cells. *Development*, *129*(18),
887 4249-4260. Retrieved from <https://www.ncbi.nlm.nih.gov/pubmed/12183377>
- 888 Barry, G., Piper, M., Lindwall, C., Moldrich, R., Mason, S., Little, E., . . . Richards, L. J. (2008).
889 Specific glial populations regulate hippocampal morphogenesis. *The Journal of
890 neuroscience : the official journal of the Society for Neuroscience*, *28*(47), 12328-12340.
891 doi:10.1523/JNEUROSCI.4000-08.2008
- 892 Basak, O., & Taylor, V. (2007). Identification of self-replicating multipotent progenitors in the
893 embryonic nervous system by high Notch activity and Hes5 expression. *The European
894 journal of neuroscience*, *25*(4), 1006-1022. doi:10.1111/j.1460-9568.2007.05370.x
- 895 Berg, D. A., Su, Y., Jimenez-Cyrus, D., Patel, A., Huang, N., Morizet, D., . . . Bond, A. M. (2019). A
896 Common Embryonic Origin of Stem Cells Drives Developmental and Adult Neurogenesis.
897 *Cell*, *177*(3), 654-668 e615. doi:10.1016/j.cell.2019.02.010
- 898 Berger, O., Li, G., Han, S. M., Paredes, M., & Pleasure, S. J. (2007). Expression of SDF-1 and CXCR4
899 during reorganization of the postnatal dentate gyrus. *Developmental neuroscience*, *29*(1-2),
900 48-58. doi:10.1159/000096210
- 901 Bertolini, J. A., Favaro, R., Zhu, Y., Pagin, M., Ngan, C. Y., Wong, C. H., . . . Wei, C. L. (2019).
902 Mapping the Global Chromatin Connectivity Network for Sox2 Function in Neural Stem Cell
903 Maintenance. *Cell stem cell*, *24*(3), 462-476 e466. doi:10.1016/j.stem.2019.02.004
- 904 Borrell, V., & Marin, O. (2006). Meninges control tangential migration of hem-derived Cajal-
905 Retzius cells via CXCL12/CXCR4 signaling. *Nature neuroscience*, *9*(10), 1284-1293.
906 doi:10.1038/nn1764
- 907 Bulfone, A., Martinez, S., Marigo, V., Campanella, M., Basile, A., Quaderi, N., . . . Ballabio, A.
908 (1999). Expression pattern of the Tbr2 (Eomesodermin) gene during mouse and chick brain
909 development. *Mechanisms of development*, *84*(1-2), 133-138. doi:10.1016/s0925-
910 4773(99)00053-2

- 911 Cerrato, V., Mercurio, S., Leto, K., Fuca, E., Hoxha, E., Bottes, S., . . . Nicolis, S. K. (2018). Sox2
912 conditional mutation in mouse causes ataxic symptoms, cerebellar vermis hypoplasia, and
913 postnatal defects of Bergmann glia. *Glia*, *66*(9), 1929-1946. doi:10.1002/glia.23448
- 914 Colom, L. V. (2006). Septal networks: relevance to theta rhythm, epilepsy and Alzheimer's disease.
915 *J Neurochem*, *96*(3), 609-623. doi:10.1111/j.1471-4159.2005.03630.x
- 916 D'Arcangelo, G., Miao, G. G., Chen, S. C., Soares, H. D., Morgan, J. I., & Curran, T. (1995). A protein
917 related to extracellular matrix proteins deleted in the mouse mutant reeler. *Nature*,
918 *374*(6524), 719-723. doi:10.1038/374719a0
- 919 de la Prida, L. M., Huberfeld, G., Cohen, I., & Miles, R. (2006). Threshold behavior in the initiation
920 of hippocampal population bursts. *Neuron*, *49*(1), 131-142.
921 doi:10.1016/j.neuron.2005.10.034
- 922 Fantes, J., Ragge, N. K., Lynch, S. A., McGill, N. I., Collin, J. R., Howard-Peebles, P. N., . . . FitzPatrick,
923 D. R. (2003). Mutations in SOX2 cause anophthalmia. *Nature genetics*, *33*(4), 461-463.
924 doi:10.1038/ng1120
- 925 Favaro, R., Valotta, M., Ferri, A. L., Latorre, E., Mariani, J., Giachino, C., . . . Nicolis, S. K. (2009).
926 Hippocampal development and neural stem cell maintenance require Sox2-dependent
927 regulation of Shh. *Nature neuroscience*, *12*(10), 1248-1256. doi:10.1038/nn.2397
- 928 Ferri, A., Favaro, R., Beccari, L., Bertolini, J., Mercurio, S., Nieto-Lopez, F., . . . Nicolis, S. K. (2013).
929 Sox2 is required for embryonic development of the ventral telencephalon through the
930 activation of the ventral determinants Nkx2.1 and Shh. *Development*, *140*(6), 1250-1261.
931 doi:10.1242/dev.073411
- 932 Ferri, A. L., Cavallaro, M., Braidà, D., Di Cristofano, A., Canta, A., Vezzani, A., . . . Nicolis, S. K.
933 (2004). Sox2 deficiency causes neurodegeneration and impaired neurogenesis in the adult
934 mouse brain. *Development*, *131*(15), 3805-3819. doi:10.1242/dev.01204
- 935 Forster, E., Tielsch, A., Saum, B., Weiss, K. H., Johanssen, C., Graus-Porta, D., . . . Frotscher, M.
936 (2002). Reelin, Disabled 1, and beta 1 integrins are required for the formation of the radial
937 glial scaffold in the hippocampus. *Proceedings of the National Academy of Sciences of the
938 United States of America*, *99*(20), 13178-13183. doi:10.1073/pnas.202035899
- 939 Fotaki, V., Price, D. J., & Mason, J. O. (2011). Wnt/beta-catenin signaling is disrupted in the extra-
940 toes (Gli3(Xt/Xt)) mutant from early stages of forebrain development, concomitant with
941 anterior neural plate patterning defects. *The Journal of comparative neurology*, *519*(9),
942 1640-1657. doi:10.1002/cne.22592
- 943 Frotscher, M., Haas, C. A., & Forster, E. (2003). Reelin controls granule cell migration in the
944 dentate gyrus by acting on the radial glial scaffold. *Cerebral cortex*, *13*(6), 634-640.
945 doi:10.1093/cercor/13.6.634
- 946 Galceran, J., Miyashita-Lin, E. M., Devaney, E., Rubenstein, J. L., & Grosschedl, R. (2000).
947 Hippocampus development and generation of dentate gyrus granule cells is regulated by
948 LEF1. *Development*, *127*(3), 469-482. Retrieved from
949 <https://www.ncbi.nlm.nih.gov/pubmed/10631168>
- 950 Gorski, J. A., Talley, T., Qiu, M., Puellas, L., Rubenstein, J. L., & Jones, K. R. (2002). Cortical
951 excitatory neurons and glia, but not GABAergic neurons, are produced in the Emx1-
952 expressing lineage. *The Journal of neuroscience : the official journal of the Society for
953 Neuroscience*, *22*(15), 6309-6314. doi:20026564
- 954 Grove, E. A. (2008). Neuroscience. Organizing the source of memory. *Science*, *319*(5861), 288-289.
955 doi:10.1126/science.1153743

- 956 Grove, E. A., Tole, S., Limon, J., Yip, L., & Ragsdale, C. W. (1998). The hem of the embryonic
957 cerebral cortex is defined by the expression of multiple Wnt genes and is compromised in
958 Gli3-deficient mice. *Development*, *125*(12), 2315-2325. Retrieved from
959 <http://www.ncbi.nlm.nih.gov/pubmed/9584130>
- 960 Hasenpusch-Theil, K., Magnani, D., Amaniti, E. M., Han, L., Armstrong, D., & Theil, T. (2012).
961 Transcriptional analysis of Gli3 mutants identifies Wnt target genes in the developing
962 hippocampus. *Cerebral cortex*, *22*(12), 2878-2893. doi:10.1093/cercor/bhr365
- 963 Hébert, J. M., & McConnell, S. K. (2000). Targeting of cre to the Foxg1 (BF-1) locus mediates loxP
964 recombination in the telencephalon and other developing head structures. *Developmental*
965 *biology*, *222*(2), 296-306. doi:S0012-1606(00)99732-X [pii]
966 10.1006/dbio.2000.9732
- 967 Hodge, R. D., Garcia, A. J., 3rd, Elsen, G. E., Nelson, B. R., Mussar, K. E., Reiner, S. L., . . . Hevner, R.
968 F. (2013). Tbr2 expression in Cajal-Retzius cells and intermediate neuronal progenitors is
969 required for morphogenesis of the dentate gyrus. *The Journal of neuroscience : the official*
970 *journal of the Society for Neuroscience*, *33*(9), 4165-4180. doi:10.1523/JNEUROSCI.4185-
971 12.2013
- 972 Hunt, D. L., Linaro, D., Si, B., Romani, S., & Spruston, N. (2018). A novel pyramidal cell type
973 promotes sharp-wave synchronization in the hippocampus. *Nature neuroscience*, *21*(7),
974 985-995. doi:10.1038/s41593-018-0172-7
- 975 Kandel, E. R., Schwartz, J. H., & Jessell, T. M. (2000). *Principles of neural science* (4th ed.). New
976 York: McGraw-Hill, Health Professions Division.
- 977 Knierim, J. J., & Neunuebel, J. P. (2016). Tracking the flow of hippocampal computation: Pattern
978 separation, pattern completion, and attractor dynamics. *Neurobiology of Learning and*
979 *Memory*, *129*, 38-49. doi:10.1016/j.nlm.2015.10.008
- 980 Kondoh H, L.-B. R. e. b. (2016). *Sox2, Biology and Role in Development and Disease* (Vol. ISBN: 978-
981 0-12-800352-7): Elsevier, Associated Press.
- 982 Korematsu, K., & Redies, C. (1997). Expression of cadherin-8 mRNA in the developing mouse
983 central nervous system. *The Journal of comparative neurology*, *387*(2), 291-306. Retrieved
984 from <https://www.ncbi.nlm.nih.gov/pubmed/9336230>
- 985 Kwon, H. J., Ma, S., & Huang, Z. (2011). Radial glia regulate Cajal-Retzius cell positioning in the
986 early embryonic cerebral cortex. *Developmental biology*, *351*(1), 25-34.
987 doi:10.1016/j.ydbio.2010.12.026
- 988 Lee, S. M., Tole, S., Grove, E., & McMahon, A. P. (2000). A local Wnt-3a signal is required for
989 development of the mammalian hippocampus. *Development*, *127*(3), 457-467. Retrieved
990 from <https://www.ncbi.nlm.nih.gov/pubmed/10631167>
- 991 Li, G., Kataoka, H., Coughlin, S. R., & Pleasure, S. J. (2009). Identification of a transient subpial
992 neurogenic zone in the developing dentate gyrus and its regulation by Cxcl12 and reelin
993 signaling. *Development*, *136*(2), 327-335. doi:10.1242/dev.025742
- 994 Li, G., & Pleasure, S. J. (2014). The development of hippocampal cellular assemblies. *Wiley*
995 *Interdiscip Rev Dev Biol*, *3*(2), 165-177. doi:10.1002/wdev.127
- 996 Lu, M., Grove, E. A., & Miller, R. J. (2002). Abnormal development of the hippocampal dentate
997 gyrus in mice lacking the CXCR4 chemokine receptor. *Proceedings of the National Academy*
998 *of Sciences of the United States of America*, *99*(10), 7090-7095.
999 doi:10.1073/pnas.092013799

- 1000 Mangale, V. S., Hirokawa, K. E., Satyaki, P. R., Gokulchandran, N., Chikbire, S., Subramanian, L., . . .
1001 Monuki, E. S. (2008). Lhx2 selector activity specifies cortical identity and suppresses
1002 hippocampal organizer fate. *Science*, *319*(5861), 304-309. doi:10.1126/science.1151695
- 1003 Mariani, J., Favaro, R., Lancini, C., Vaccari, G., Ferri, A. L., Bertolini, J., . . . Nicolis, S. K. (2012). Emx2
1004 is a dose-dependent negative regulator of Sox2 telencephalic enhancers. *Nucleic acids*
1005 *research*, *40*(14), 6461-6476. doi:10.1093/nar/gks295
- 1006 Mercurio, S., Serra, L., Motta, A., Gesuita, L., Sanchez-Arrones, L., Inverardi, F., . . . Nicolis, S. K.
1007 (2019). Sox2 Acts in Thalamic Neurons to Control the Development of Retina-Thalamus-
1008 Cortex Connectivity. *iScience*, *15*, 257-273. doi:10.1016/j.isci.2019.04.030
- 1009 Meyer, G., Cabrera Socorro, A., Perez Garcia, C. G., Martinez Millan, L., Walker, N., & Caput, D.
1010 (2004). Developmental roles of p73 in Cajal-Retzius cells and cortical patterning. *The*
1011 *Journal of neuroscience : the official journal of the Society for Neuroscience*, *24*(44), 9878-
1012 9887. doi:10.1523/JNEUROSCI.3060-04.2004
- 1013 Meyer, G., Gonzalez-Arnay, E., Moll, U., Nemajerova, A., Tissir, F., & Gonzalez-Gomez, M. (2019).
1014 Cajal-Retzius neurons are required for the development of the human hippocampal fissure.
1015 *J Anat*, *235*(3), 569-589. doi:10.1111/joa.12947
- 1016 Meyer, G., Schaaps, J. P., Moreau, L., & Goffinet, A. M. (2000). Embryonic and early fetal
1017 development of the human neocortex. *The Journal of neuroscience : the official journal of*
1018 *the Society for Neuroscience*, *20*(5), 1858-1868. Retrieved from
1019 <https://www.ncbi.nlm.nih.gov/pubmed/10684887>
- 1020 Miles, R., & Wong, R. K. (1983). Single neurones can initiate synchronized population discharge in
1021 the hippocampus. *Nature*, *306*(5941), 371-373. doi:10.1038/306371a0
- 1022 Mimura-Yamamoto, Y., Shinohara, H., Kashiwagi, T., Sato, T., Shioda, S., & Seki, T. (2017).
1023 Dynamics and function of CXCR4 in formation of the granule cell layer during hippocampal
1024 development. *Sci Rep*, *7*(1), 5647. doi:10.1038/s41598-017-05738-7
- 1025 Moser, M. B., & Moser, E. I. (1998). Functional differentiation in the hippocampus. *Hippocampus*,
1026 *8*(6), 608-619. doi:10.1002/(SICI)1098-1063(1998)8:6<608::AID-HIPO3>3.0.CO;2-7
- 1027 Muotri, A. R., Marchetto, M. C., Coufal, N. G., Oefner, R., Yeo, G., Nakashima, K., & Gage, F. H.
1028 (2010). L1 retrotransposition in neurons is modulated by MeCP2. *Nature*, *468*(7322), 443-
1029 446. doi:10.1038/nature09544
- 1030 Naruse, I., Ueta, E., Sumino, Y., Ogawa, M., & Ishikiriya, S. (2010). Birth defects caused by
1031 mutations in human GLI3 and mouse Gli3 genes. *Congenit Anom (Kyoto)*, *50*(1), 1-7.
1032 doi:10.1111/j.1741-4520.2009.00266.x
- 1033 Panaliappan, T. K., Wittmann, W., Jidigam, V. K., Mercurio, S., Bertolini, J. A., Sghari, S., . . .
1034 Gunhaga, L. (2018). Sox2 is required for olfactory pit formation and olfactory neurogenesis
1035 through BMP restriction and Hes5 upregulation. *Development*, *145*(2).
1036 doi:10.1242/dev.153791
- 1037 Ragge, N. K., Lorenz, B., Schneider, A., Bushby, K., de Sanctis, L., de Sanctis, U., . . . Fitzpatrick, D. R.
1038 (2005). SOX2 anophthalmia syndrome. *Am J Med Genet A*, *135*(1), 1-7.
1039 doi:10.1002/ajmg.a.30642
- 1040 Roelink, H. (2000). Hippocampus formation: an intriguing collaboration. *Current biology : CB*,
1041 *10*(7), R279-281. Retrieved from <http://www.ncbi.nlm.nih.gov/pubmed/10753739>
- 1042 Rogers, N., Cheah, P. S., Szarek, E., Banerjee, K., Schwartz, J., & Thomas, P. (2013). Expression of
1043 the murine transcription factor SOX3 during embryonic and adult neurogenesis. *Gene Expr*
1044 *Patterns*, *13*(7), 240-248. doi:10.1016/j.gep.2013.04.004

- 1045 Sisodiya, S. M., Ragge, N. K., Cavalleri, G. L., Hever, A., Lorenz, B., Schneider, A., . . . Fitzpatrick, D.
1046 R. (2006). Role of SOX2 mutations in human hippocampal malformations and epilepsy.
1047 *Epilepsia*, 47(3), 534-542. doi:10.1111/j.1528-1167.2006.00464.x
- 1048 Srinivas, S., Watanabe, T., Lin, C. S., William, C. M., Tanabe, Y., Jessell, T. M., & Costantini, F.
1049 (2001). Cre reporter strains produced by targeted insertion of EYFP and ECFP into the
1050 ROSA26 locus. *BMC developmental biology*, 1, 4. doi:10.1186/1471-213x-1-4
- 1051 Swanson, L. W., & Cowan, W. M. (1977). An autoradiographic study of the organization of the
1052 efferent connections of the hippocampal formation in the rat. *The Journal of comparative*
1053 *neurology*, 172(1), 49-84. doi:10.1002/cne.901720104
- 1054 Theil, T., Alvarez-Bolado, G., Walter, A., & Ruther, U. (1999). Gli3 is required for Emx gene
1055 expression during dorsal telencephalon development. *Development*, 126(16), 3561-3571.
1056 Retrieved from <https://www.ncbi.nlm.nih.gov/pubmed/10409502>
- 1057 Theil, T., Aydin, S., Koch, S., Grotewold, L., & Ruther, U. (2002). Wnt and Bmp signalling
1058 cooperatively regulate graded Emx2 expression in the dorsal telencephalon. *Development*,
1059 129(13), 3045-3054. Retrieved from <https://www.ncbi.nlm.nih.gov/pubmed/12070081>
- 1060 Traub, R. D., Jefferys, J. G. R., & Whittington, M. A. (1999). *Fast oscillations in cortical circuits*.
1061 Cambridge, Mass.: MIT Press.
- 1062 Tronche, F., Kellendonk, C., Kretz, O., Gass, P., Anlag, K., Orban, P. C., . . . Schutz, G. (1999).
1063 Disruption of the glucocorticoid receptor gene in the nervous system results in reduced
1064 anxiety. *Nature genetics*, 23(1), 99-103. doi:10.1038/12703
- 1065 Venkatesan, K., Liu, Y., & Goldfarb, M. (2014). Fast-onset long-term open-state block of sodium
1066 channels by A-type FHF mediates classical spike accommodation in hippocampal
1067 pyramidal neurons. *The Journal of neuroscience : the official journal of the Society for*
1068 *Neuroscience*, 34(48), 16126-16139. doi:10.1523/JNEUROSCI.1271-14.2014
- 1069 Visel, A., Blow, M. J., Li, Z., Zhang, T., Akiyama, J. A., Holt, A., . . . Pennacchio, L. A. (2009). ChIP-seq
1070 accurately predicts tissue-specific activity of enhancers. *Nature*, 457(7231), 854-858.
1071 doi:10.1038/nature07730
- 1072 Wei, C. L., Nicolis, S. K., Zhu, Y., & Pagin, M. (2019). Sox2-Dependent 3D Chromatin Interactomes
1073 in Transcription, Neural Stem Cell Proliferation and Neurodevelopmental Diseases. *J Exp*
1074 *Neurosci*, 13, 1179069519868224. doi:10.1177/1179069519868224
- 1075 Witter, M. P., & Amaral, D. G. (2004). Hippocampal formation. In E. Paxinos (Ed.), *The Rat Nervous*
1076 *System* (third ed., pp. 635-704): Elsevier.
- 1077 Yang, A., Walker, N., Bronson, R., Kaghad, M., Oosterwegel, M., Bonnin, J., . . . Caput, D. (2000).
1078 p73-deficient mice have neurological, pheromonal and inflammatory defects but lack
1079 spontaneous tumours. *Nature*, 404(6773), 99-103. doi:10.1038/35003607
- 1080 Zhong, S., Ding, W., Sun, L., Lu, Y., Dong, H., Fan, X., . . . Wang, X. (2020). Decoding the
1081 development of the human hippocampus. *Nature*, 577(7791), 531-536.
1082 doi:10.1038/s41586-019-1917-5
1083